A rapid groundwater circulation system inferred from temporal water dynamics and isotopes in a typical alluvial-fluvial fan of the Nalenggele River in arid Qaidam Basin, China

Hongbing Tan[1], Yu Zhang[2], Wenbo Rao[3], Wanquan Ta[4], Hongye Guo[5], Shicheng Lu[1], and Peixing Cong[1]

[1]Hohai University
[2]School of Earth Sciences and Engineering, Hohai University
[3]Institute of Isotope Hydrology, College of Earth Sciences and Engineering, Hohai University
[4]Cold and Arid Regions Environmental and Engineering Research Institute, Chinese Academy of Sciences
[5]Qinghai Province Hydrogeology and Engineering Geology Environmental Institute of Geological Survey

November 22, 2022

Abstract

A rapid groundwater recharge and circulation system has developed in Qaidam Basin, China. Stable H and O isotopes were monthly sampled in both river water and groundwater, and water table fluctuations were monitored over a complete seasonal cycle from dry-season to wet-season conditions in the Nalenggele River catchment in Qaidam Basin. The main goals are to demonstrate and explain rapid circulation in the groundwater system. A distinct seasonal fluctuation of the water table with associated stable isotopic variations can be observed in the alluvial-fluvial fan of the Nalenggele River catchment. During the wet season, replenishment of the aquifer results in a rising water table rises. The recharge mechanism appears to be related to the coincidence of several favorable hydrological conditions: an abundant recharge water source from summer precipitation and glacial-snow melt in the high Kunlun mountains, large-scale active faults, a volcanic crater and other macro-structures that act as favorable recharge conduits, the large hydraulic head from recharge areas to the alluvial-fluvial fan, and the presence of over 100 m of unconsolidated sand and gravel acting as the main aquifer. Warming climate is expected to increase precipitation and to accelerate melting of glaciers in the Kunlun Mountains, increasing recharge and leading to rapid rise in the water table in the alluvial-fluvial fan. Increased recharge in the future will provide water of improved quality to the Qaidam Basin, and will allow management of land in ways that reduce soil salinity and alkalinity.

1

1   **A rapid groundwater circulation system inferred from temporal water dynamics and**

2   **isotopes in a typical alluvial-fluvial fan of the Nalenggele River in arid Qaidam Basin, China**

3

4   **Hongbing Tan*[1], Yu Zhang[1], Wenbo Rao*[1], Wanquan Ta[2], Hongye Guo[2], Shicheng Lu[1], Peixing Cong[1]**

5   1) School of Earth Sciences and Engineering, Hohai University, Nanjing, China;

6   2) Qinghai Province Hydrogeology and Engineering Geology Environmental Institute of Geological Survey, Xining,

7   China;

8   3) Cold and Arid Regions Environmental and Engineering Research Institute, Chinese Academy of Sciences,

9   Nanzhou, China

10

11   * Corresponding author: Hongbing Tan (tan815@sina.com); Wenbo Rao (raowenbo@163.com)

12

13   **Key Points:**

14   • A rapid groundwater circulation system has been approved.

15   • Water source, macro-structures and large hydraulic head governing rapid circulation.

16   • Warming climate is expected to increase recharge groundwater.

17
18
19
20
21
22
23
24
25
26

Abstract

A rapid groundwater recharge and circulation system has developed in Qaidam Basin, China. Stable H and O isotopes were monthly sampled in both river water and groundwater, and water table fluctuations were monitored over a complete seasonal cycle from dry-season to wet-season conditions in the Nalenggele River catchment in Qaidam Basin. The main goals are to demonstrate and explain rapid circulation in the groundwater system. A distinct seasonal fluctuation of the water table with associated stable isotopic variations can be observed in the alluvial-fluvial fan of the Nalenggele River catchment. During the wet season, replenishment of the aquifer results in a rising water table rises. The recharge mechanism appears to be related to the coincidence of several favorable hydrological conditions: an abundant recharge water source from summer precipitation and glacial-snow melt in the high Kunlun mountains, large-scale active faults, a volcanic crater and other macro-structures that act as favorable recharge conduits, the large hydraulic head from recharge areas to the alluvial-fluvial fan, and the presence of over 100 m of unconsolidated sand and gravel acting as the main aquifer. Warming climate is expected to increase precipitation and to accelerate melting of glaciers in the Kunlun Mountains, increasing recharge and leading to rapid rise in the water table in the alluvial-fluvial fan. Increased recharge in the future will provide water of improved quality to the Qaidam Basin, and will allow management of land in ways that reduce soil salinity and alkalinity.

1 Introduction

Many studies conclude that groundwater should be very old in arid or semi-arid basins, e.g. most basins or plateaus in northern China and deserts (Ma et al., 2009; Jiang et al., 2019) . Globally, there is a growing body of evidence suggesting that many of Earth's aquifers contain 'fossil' groundwater that was recharged more than 12,000 years ago, and only a very small portion of groundwater was recharged in the last 50 years (Gleeson et al., 2016; Jasechko et al., 2017; Smerdon et al., 2017). However, in most basins, rainwater also finds its way through macropores and preferential pathways to shallow unconfined aquifers within hours of falling (Glenn et al., 2015; Hartmut et al., 2019). At present, the nature of rapid groundwater circulation or even seasonal recharge in arid basins that are remote from recharge sources remains unclear. The mechanisms or conceptual models governing the rapid recharge need to be further investigated. In addition, the global volume and distribution of groundwater less than 50 years old, which is the most vulnerable

58   to global climate change, are unknown (Gleeson et al., 2016). Given the expected challenges arising

59   from future global and regional climate changes, it is important to improve the understanding of

60   aquifers dominated by young groundwater. Accurate assessment of water resources and clear

61   understanding of the hydrology in such aquifers will be important to future management of

62   groundwater use, of ecological changes in vulnerable environments, and of secondary hazards

63   resulting from rising groundwater levels.

64   The Nalenggele River (NR) catchment was selected as the study area. It is a typical large river

65   draining the high and cold area of the northern slope of the eastern Kunlun Mountains (KM) and

66   ending in the western Qaidam Basin (QB) (Fig. 1). In this region, sources of groundwater recharge,

67   spatial and temporal variations of runoff and interactions between groundwater and stream flow are

68   very complex and remain unclear. There have been a few previous studies on a surface-groundwater

69   system in the NR catchment and adjacent area in the Golmud and Nomhon River catchments (Xiao

70   et al. 2017a and b; Xu et al., 2017). These previous studies found that the groundwater systems

71   resembled a typical mountain-basin system. However, it remains unclear why water tables at depths

72   of 10 to 50m or even deeper fluctuate so greatly under natural conditions. Such changes are difficult

73   to explain with an ancient recharge model. In the absence of monthly monitoring data, it is not

74   known whether seasonal changes in water table depth are associated with changes in stable H and

75   O isotopes in groundwater. The previous conclusions were mainly dependent on ^{14}C to determine

76   the age of groundwater. However, neither methods are capable of resolving differences among

77   seasonal pulses of recharge. It is of critical importance to confirm rapid (annual, seasonal or even

78   daily) recharge of groundwater in an arid basin. This will directly relate to accurate assessment of

79   groundwater resources and their management. Thus, a systematic and detailed study is necessary

80   for groundwater systems like those in the extremely arid QB, particularly in the alluvial-fluvial fan

81   (AFF) of the NR catchment where groundwater appears to be abundant.
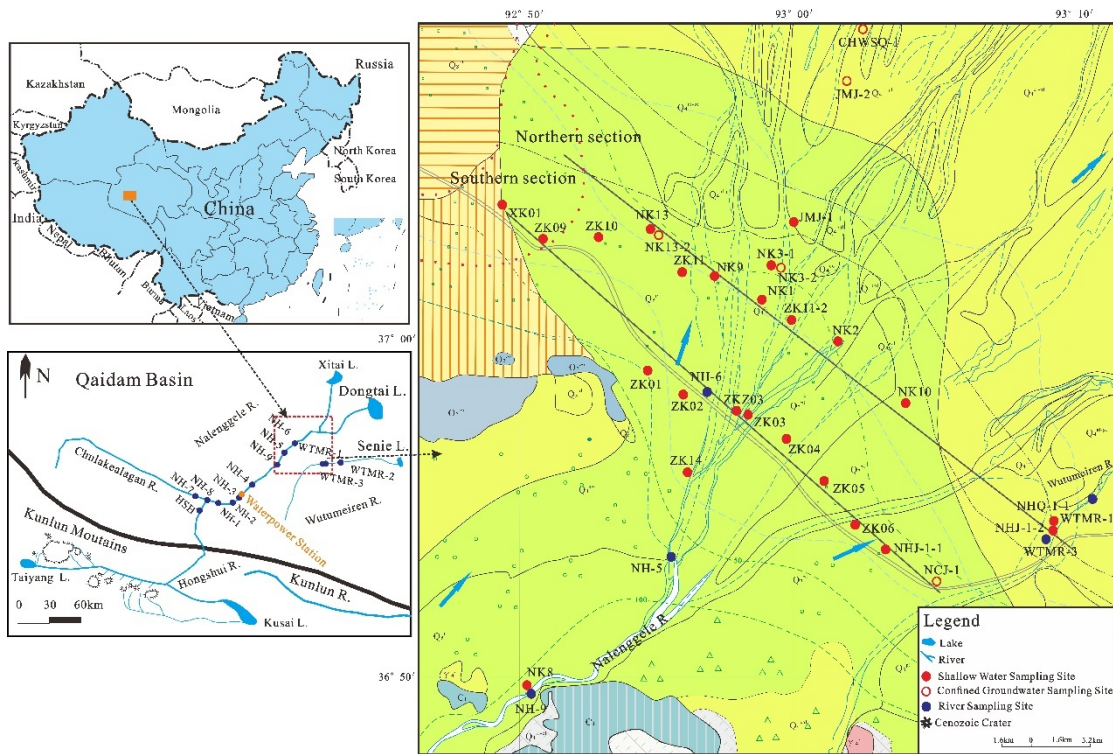
82

83

84

85

86

87

88

Figure 1 Simplified hydrogeologic map of the Nalenggele River catchment and location of the sampling sites (Two monitoring sections: southern and northern sections are located around the centre and near the northern edge of an alluvial-fluvial fan).

In recent years, the prospect of warming arising from climate change has led to concerns over large-scale shrinkage of glaciers and subsurface permafrost degradation in the source regions of rivers in the Tibetan Plateau (Cheng and Wu, 2007; Yang et al., 2007; Ge et al., 2008; Zhang et al., 2013). Therefore, Tibet has become a focus of global interest as hydrologists assess the variation of surface runoff and recharge in the main river catchments with the aim of predicting future changes. Recent observations show significant warming on the Tibetan Plateau during the past several decades (Chen et al., 2013; Gao et al., 2015; You et al., 2015), and climate models predict warming will continue in the future (Rangwala et al., 2010; Ji and Kang, 2013; Zhu et al., 2013; Sun et al., 2015). Recent reports state that the glacial area has declined by 15% and the permafrost area has decreased by 16%, whereas the lake area has increased from 40000 km^2 to 47400 km^2 over the past 50 years in the Tibetan Plateau (Li et al., 2020). Satellite gravity data together with multiple hydrologic models provide clear evidence of increasing groundwater storage in the eastern Tibetan Plateau, again reflecting increased abundance of glacial meltwater (Xiang et al., 2016). In particular, the GRACE data analysis discovered that the variation of total water storage (TWS) showed a

108　　　distinct upward trend in QB (Jiao et al., 2015; Wang et al., 2018). Correspondingly, the most

109　　　significant climate warming is found in the QB (Chen et al., 2013; Wang et al., 2014; Kuang et al.,

110　　　2016). From 1961 to 2010, the annual mean temperature in the QB increased by 0.53°C decade^{-1}

111　　　and the annual mean temperature increased about 2.65°C (Wang et al., 2014). Without doubt, such

112　　　warming will lead to significant changes in hydrology and water resources on the Tibetan Plateau,

113　　　particularly in arid QB.

114　　　　Research interest in the response of glaciers to global warming is not confined to the Tibetan

115　　　Plateau. The topic is being addressed in other regions (e.g. Mark, 2003; Bijeesh et al., 2017), but is

116　　　in its infancy, and many aspects remain to be studied (Aude et al., 2019). In alpine cold-arid basins,

117　　　the prevalent viewpoint is that massive recharge happened as a result of melting of ice just after the

118　　　Last Glacial Maximum (LGM) (Post et al., 2013; Salamon, 2016). Some studies concluded that the

119　　　depleted isotopic signatures of groundwater in North China Plain indicate recharge of palaeo-waters

120　　　during glacial–interglacial transitional periods (Chen et al., 2003; Currell et al., 2010; Gates et al.,

121　　　2008). However, it remains to be confirmed whether global recharge after the LGM indeed occurred.

122　　　Glacier meltwater has commonly been suggested as a substantial source of recharge for nearby

123　　　porous, karstic, or fractured-rock aquifers. Malard et al. (2016) identified a karstic aquifer under the

124　　　Fonds glacier (Swiss-French border) and determined that for karst in Swiss alpine areas above 2500

125　　　m, recharge is due both to precipitation and to glacier melting. Another mode of rapid groundwater

126　　　recharge may occur in fractured-rock aquifers or faults acting as conduits, but is less frequently

127　　　observed. Chen and Wang (2009) concluded that the 2003 M6.1 earthquake in the Hexi Corridor in

128　　　China caused local groundwater to be greatly increased recharge from the Qilian Mountains through

129　　　numerous seismically-active faults that crisscross the Corridor. In summary, traditional hydrological

130　　　theories proposed that groundwater recharge is a very slow process in arid basins, occurring far

131　　　away from water sources, and did not allow for dominantly young groundwater with distinct pulses

132　　　of annual or seasonal recharge in arid basins. This may indeed apply in arid basins with almost no

133　　　recharge from local precipitation, but has not been demonstrated in all cases, in particular for arid

134　　　basins adjacent to high-cold mountains.

135　　　　Isotopes of hydrogen and oxygen have been widely used in hydrologic studies of water circulation

136　　　processes (Clark et al.1997; Kendall et al., 1998; Tian et al., 2007; Pradeep et al., 2010). The

137　　　radioisotope ^{222}Rn has also been used to identify groundwater discharge to rivers (Smerdon et al.

138　　　2012; Yael et al., 2015; Su et al. 2015; Xu et al., 2017). Transient activities of radon isotopes are

usually high in groundwater that has been in contact with rock bearing parent nuclides (Krishnaswami et al., 1982). High Rn concentrations are focused near points of discharge from fractures in certain granitoids (Gascoyne et al., 1993). Thus, ^{222}Rn can be used to identify buried faults acting as conduits for groundwater. In addition, helium isotope ratios (^{3}He/^{4}He) are excellent natural tracers for locating deep faults and tracing groundwater circulation along deep faults in the Earth's crust (Gascoyne et al., 1993; Kennedy et al., 1985; Weiss, 1971; Tolstinkhin et al., 1996; Kennedy and Matthijs, 2006).

In this study, stable H and O isotopes were monitored in river water and AFF groundwater of the NR catchment at monthly intervals over a complete seasonal cycle from dry-season to wet-season conditions. Tritium and ^{222}Rn were also measured for water under base conditions in the dry season in April. In addition, several years' observations of water table fluctuation at monthly time-scale are discussed. The study focused on the following goals: 1) determining relationships between spatial and temporal fluctuation of water tables and stable isotopic variations over a complete seasonal cycle from dry-season to wet-season conditions; 2) demonstrating rapid circulation in the groundwater system and determining the recharge mechanism; and 3) predicting the effects of future climate warming on water table fluctuations and groundwater storage.

2 Study area and methods

2.1 Hydrology and geography

The lower reach of the NR catchment is located in the southwest part of QB and is managed by Golmud city in Qinghai province, China (Fig. 1). The climate is a typical inland dry climate with very scarce precipitation, strong wind and intense evaporation. The winter is very long but the summer is short with a large diurnal temperature variation. According to data from Xiaozaohuo meteorological station, precipitation occurs mainly between late May and September, and averages 29.8mm annually. The annual average potential evaporation is nearly 100 times the total precipitation. The average annual temperature ranges from 2.6 to 4.3 °C and the highest monthly average temperature (ranging from 15.1 to 18.7℃) generally occurs in July. No meteorological records exist for the high mountainous parts of the NR catchment because of the harsh natural conditions, but the glaciers and snow are widespread, and precipitation, also dominantly in summer, should be much higher than in the lower parts of the basin. Large storms and floods frequently occur in summer in the mountains. The mountains are uninhabited, and the lower reach of the basin

170   is sparsely inhabited, so that the eco-environment remains in a nearly natural state. However, a

171   large water control project to be built in the coming 10 years in the middle reach of NR will most

172   likely affect natural hydrology, hydrogeology and water resources in the lower reach.

173   The NR, which rises in the eastern KM, is the largest river in QB with a length of over 435km

174   and a catchment area of about 21898km^2. No flow gauges are installed on the river, so that

175   systematic hydrometric data are unavailable. An estimate of the total annual runoff is about 10^9

176   m^3/a (Wang et al., 2008). Field observations in 2019 (this study) indicated that the river runoff in

177   the mountains shows a large seasonal change. In winter, base flow is maintained by mountain

178   spring discharge. In spring and early summer, flow is supplied by melt water from snow and

179   glaciers. Both melt water and runoff from summer precipitation contribute to flow during the

180   humid season, June to September. In particular, frequent heavy rainstorms strongly affect summer

181   runoff in August and September. According to field estimates, the base flow in April seems to be

182   similar in volume in the two largest tributaries, the Hongshui River (HR) and Chulakealagan River

183   (CR) in the upper catchment. However, the runoff in the HR is distinctly larger than that in the CR

184   in July. The mainstream is generally dry at the driest time of the year from November to April. At

185   other times, river water discharges into the basin, but even in summer season when flow is greatest,

186   over 70% of surface water infiltrates before reaching the basin (Wang et al., 2008). In the wet

187   season, groundwater discharged from springs at the downgradient limit of the AFF converges into

188   streams that flow north into the QB, terminating in salt lakes (Fig. 1).

189   **2.2 Basic hydrogeology of groundwater system**

190   The upper catchment of the NR is located in the northern slope of eastern KM at elevations

191   from 2,800 to over 5,000 m above sea level (a.s.l.). Intense neotectonic activity is expressed as a

192   set of high-angle thrust faults parallel to the range front, a secondary set of tensile faults

193   approximately perpendicular to the thrust faults, and a set of volcanic vents. Some faults extend to

194   lower parts of the basin (Fig. 2). Part of the melt water and precipitation inform the high elevations

195   converges into surface water in streams and mountain lakes. Some surface water infiltrates through

196   faults, fissures and volcanic edifices to a fractured-rock aquifer in the mountains. The groundwater

197   developed in the high mountains flows towards the basin, locally discharge into rivers where

198   favorable geological and geomorphological conditions exist. The river and the fractured-rock

199   aquifer are closely connected, and exchange water over the entire hard-rock stream bed. According

200   to aquifer types, physical properties and water dynamics, four kinds of aquifer are present:

fractured bedrock, karst, consolidated clastic sedimentary rock with intergranular porosity in addition to fracture porosity, and unconsolidated sediment. A fifth occurrence takes the form of ice in frozen soil and rock at high latitudes. Since the Quaternary period, the western QB in front of eastern KM has been subsiding, resulting in the deposition of thick, unconsolidated sediment sequences in the basin. These deposits from a set of large, porous aquifers with great water-yield potential. The maximum thickness of the phreatic aquifer in the mountain region is probably tens of meters, while the total thickness of the phreatic aquifer and multiple confined aquifers in the alluvial-fluvial fan and alluvial-fluvial plain is hundreds of meters. The confined groundwater may well up locally to replenish the upper phreatic aquifers or discharge direct to the surface as artesian flow through deep buried faults or "sky windows". The water table lies about 50 m below the surface at the mountain front, over 10 m in the center of the AFF, and intersects the surface at the foreland of the AFF mountains (Table 1). The aquifer system is over 100-200 m thick at the center of the fan. The AFF of the NR is the largest fan in the QB, and contains one of the richest groundwater resources in the area. The groundwater quality is excellent in all aquifers of the AFF and is almost undisturbed by development at present.
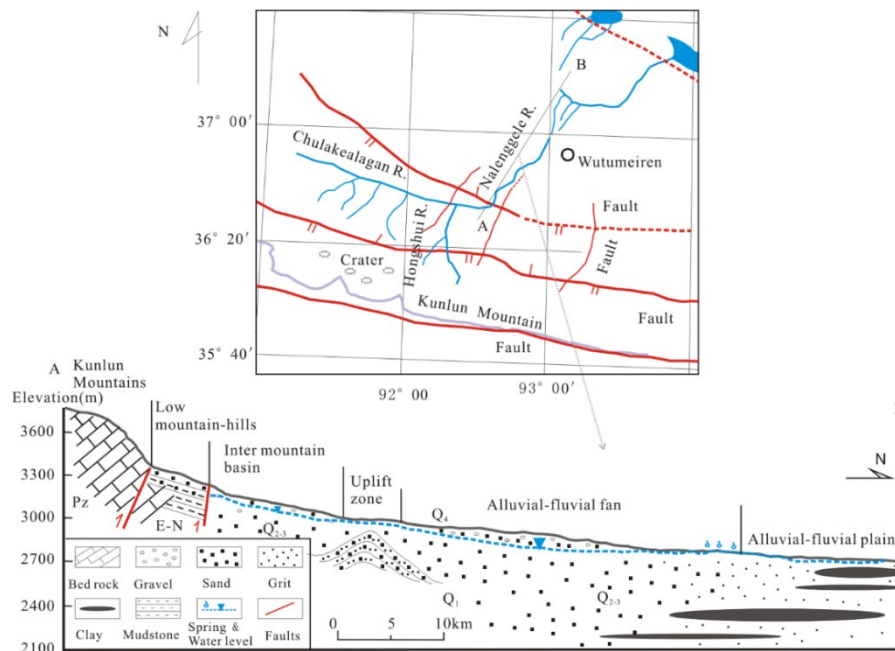

Figure 2 Simplified tectonic map of the source and upper reaches in the Nalenggele River and basic hydrogeologic section (A-A line)

Table 1 Basic information of sampling sites (well or spring)

Site	Sample number	Elevation /m	Well Depth/m	Type	Water yield/m³/d	Water table/m	Aquifer thickness /m	Main lithology
Mountain	SDJ-1	3266		CW				Sands, gravel
Southern Section	XK01	2902		PW		22.86		Sands, gravel
	ZK10	2904	121.15	PW	5279	34.56	86.59	Sands, gravel
	ZK09	2905	120.10	PW	4761	33.93	86.17	Sands, gravel
	ZK01*	2940	150.3	PW	5495	32.23	107.23	Sands, gravel
	ZK02	2878	151.5	PW	8199	15.97	125.91	Sands, gravel
	ZK14	2974	150.60	PW	6307	19.29	120.37	Sands, gravel
	ZKZ03	2929	150.0	PW		27.15		Sands, gravel
	ZK03*	2924	150.0	PW	9685	26.97	119	Sands, gravel
	ZK04	2927	150.60	PW	8934	24.08	121.77	Sands, gravel
	ZK05*	2941	150.28	PW	9832	26.84	123.44	Sands, gravel
	ZK06*	2945	150.20	PW	9331	26.655	118.65	Sands, gravel
	NK8	3073	31.40	PW	1900	3.34	15.10	Sands, gravel
	NHJ-1-1	2925	70	CW		5.0		Sands, gravel
	NCJ-1	2909		CW		5.0		Sands, gravel
Northern Section	NK13	2876	250.2	PW	3675	8.06	212.7	Sands, gravel
	ZK11	2876	120.00	PW	8588	8.48	108.6	Sands, gravel
	NK9	2880	200.75	PW	2400	6.53	188.76	Sands, gravel, mud
	NK1	2879	251.00	PW	4259	7.79	222.28	Sands, gravel
	JMJ-1	2871	10	CG		0		Sands, grit
	JMJ-2	2826	10	CG		0		Sands, grit
	CHWSQ-1	2823		Spring		0		Sands, grit
	NK3-1*	2877	251	PW		1.19	92.29	Sands, gravel, mud
	NK3-2		300	CG		0.35	170.35	
	ZK11-2	2885		PW		8.57		Sands, gravel
	NK2	2884	198.00	PW	1252	3.94	194.18	Sands, grit, mud
	NK10*	2886	250.63	PW	4242	0.45	92.55	Sands, gravel
	NHQ-1-1	2860		Spring		0		Sands, gravel
	NHJ-1-2	2858	15	CW		3.0		Sands, gravel

*Automatic gauge was installed to record groundwater table. CW-Civil well; PW-Phreatic groundwater; CG-Confined groundwater. Blank space means no data available.

223

224

225

226

227

228

2.3 Sampling strategy and measurements

Groundwater and river water samples were collected from early April to October (April, June, July, September and October) in 2019. Tritium, He isotopes and ^{222}Rn measurements of groundwater were made only on samples collected in April, which can represent the sample under the base condition. The monthly river samples were collected simultaneously (same period with groundwater sample) at sites from the high mountain zone to the northern edge of the AFF. Two monitoring sections for groundwater sampling and water table measurement are roughly perpendicular to the river channel around the AFF. The southern monitoring section cut through the center of the fan and included some wells near the mountain front. The northern monitoring section was located near the northern edge of the fan and included some shallow wells and springs near the edge of the fan (Fig. 1). Before sampling, the depth to the water table was measured first (some wells had automatic water-level meters installed). Given the typical well depths (150-250m) and depths to the water table (>10m), it was impractical to pump the wells dry before sampling. Instead, a special instrument (depth-setting sampler) was inserted at least 50 m below the water table to take the groundwater samples. The tritium, radon and inert gas samples were collected from water extracted by a bore-hole turbine pump driven by a high-power electromotor, after pumping for two hours in order to avoid atmospheric contamination to the greatest extent possible

Samples for stable isotopic analysis were sealed tightly in special thick plastic bottles. At the time of sampling, the electrical conductivity, pH, and temperature were measured using standard hand-held calibrated field meters. Because of its short half-life, ^{222}Rn was analyzed in the field using a DURRIDGE USA (RAD 7) radon detector. Five measurements were taken over 1 to 2 hours; the first was discarded, and the remaining four were averaged to yield the reported measurement. The detection limit was 0.4000 cpm/pCi/L. Data were accepted if the uncertainty of measurements fell within ±25% of the mean (confidence level: 95 percent). The measurement time was extended if the range of the readings exceeded ± 25%.

Measurements of stable H and O isotopes were performed at the State Key Laboratory of Hydrology-Water Resources and Hydraulic Engineering, Hohai University, Nanjing. The ^{2}H/^{1}H and ^{18}O/^{16}O ratios were measured on a MAT253 mass spectrometer, and the results are reported relative to VSMOW with analytical precisions (1σ) of ±1‰ to 2‰ and ±0.2‰ to 0.3‰, respectively. For the determination of the tritium content in groundwater, the water samples were concentrated through electrolysis and then measured by a low-background liquid scintillation counting (Tri-Carb

260 3170 TR/SL), and the results were expressed as absolute concentrations in tritium units (TU) with

261 a precision (1σ) of ±0.8 TU or better, and a detection limit of 0.2 TU. Analytical techniques and

262 instrumentation for He isotope analyses were similar to those described by Ye et al. (2007). He

263 isotopes were measured using a MM5400 mass spectrometer in the Laboratory of Gas Geochemistry

264 (Lanzhou), Institute of Geology and Geophysics, Chinese Academy of Sciences. $^3He/^4He$ ratios

265 were reproducible in duplicate analyses to ±1%. All the results are listed in Table 2-3.

266

267 **Table 2** Stable H and O and radio tritium isotopic data of groundwater samples in different months

Site	Sam. No.	April			June		July		September		Octobet		December		Std	
		δD‰	δ^{18}O‰	T (TU)	δD‰	δ^{18}O‰	δD‰	δ^{18}O‰	δD‰	δ^{18}O‰	δD‰	δ^{18}O‰	δD‰	δ^{18}O‰	δD	δ^{18}O
Southern Section	XK01			8.22			-68.3	-9.37	-69.9	-10.31	-69.8	-10.09			0.7	0.40
	ZK10	-58.2	-9.22	19.07	-56.3	-8.24	-55.5	-7.93	-57.8	-9.42	-52.9	-6.98	-58.0	-9.54	1.9	0.92
	ZK09	-60.7	-9.14	8.25	-59.8	-9.16	-56.1	-7.61	-60.1	-9.41	-59.3	-9.09	-59.7	-9.26	1.5	0.60
	ZK01	-58.2	-9.31	15.44	-59.6	-9.19	-51.2	-6.27	-58.6	-9.50	-51.4	-6.95	-60.0	-9.93	3.7	1.39
	ZK02	-57.6	-9.21	13.39	-57.3	-7.94	-58.2	-9.16	-58.7	-9.36	-53.4	-7.87	-58.4	-8.95	1.8	0.61
	ZK14	-59.6	-9.40	10.33	-57.2	-8.88	-57.6	-9.45	-57.4	-9.41	-56.4	-9.32			1.0	0.21
	ZKZ03	-54.1	-8.60	9.20	-54.0	-8.50	-56.0	-8.85			-46.3	-5.94	-53.8	-8.17	3.4	1.06
	ZK03	-59.7	-9.31	8.71	-56.8	-7.96	-55.3	-8.34	-54.5	-8.80			-57.2	-8.96	1.8	0.47
	ZK04	-59.3	-9.36	8.14	-58.2	-9.04	-52.0	-7.21			-56.8	-7.77	-61.9	-9.63	3.3	0.95
	ZK05	-55.7	-8.41	8.56	-54.9	-7.94	-59.6	-9.00			-57.8	-8.91			1.8	0.43
	ZK06	-58.4	-9.12	8.22	-57.9	-8.47	-60.1	-8.82	-59.2	-9.18	-58.8	-9.13	-58.9	-9.65	0.7	0.36
	NK8			16.25			-50.2	-6.89					-56.1	-9.30	2.9	1.21
	NHJ-1-1	-54.9	-8.65	8.08			-56.0	-8.88							0.5	0.11
	NCJ-1	-55.2	-8.63	8.42			-49.6	-6.51							2.8	1.06
Nothern Section	NK13	-60.2	-9.14	7.85	-59.6	-9.16	-59.3	-9.02	-60.2	-9.29	-59.6	-9.41	-58.8	-9.55	0.5	0.18
	ZK11	-53.9	-8.70	18.94			-54.1	-8.57	-54.7	-8.88	-51.7	-7.60	-57.5	-8.51	1.9	0.44
	NK9	-53.1	-8.37	12.47	-53.2	-7.87	-54.8	-8.43			-50.3	-6.54	-54.7	-8.11	1.6	0.69
	NK1	-53.5	-8.51	10.15			-53.8	-8.67					-51.1	-9.01	1.2	0.21
	JMJ-1			10.68			-54.9	-8.15			-54.4	-8.76			0.2	0.30
	JMJ-2			8.62			-51.0	-6.20			-57.1	-9.03			3.0	1.41
	CHWSQ-1			bd			-53.1	-5.82			-63.4	-9.70			5.1	1.94
	NK3-1	-56.2	-8.85	8.62	-52.5	-7.77	-48.2	-5.91			-53.7	-8.53			2.9	1.14
	NK3-2	-55.4	-8.91	12.76	-54.6	-8.54	-57.5	-8.58			-54.9	-8.57			1.1	0.15
	ZK11-2	-53.3	-8.27	9.02			-58.1	-8.77							2.4	0.25
	NK2	-53.5	-8.30	7.45			-55.3	-8.85							0.9	0.27
	NK10	-53.2	-8.56	8.21	-53.6	-8.62	-51.1	-6.78	-53.2	-8.85	-50.0	-6.91			1.4	0.90
	NHQ-1-1	-56.4	-8.78	14.02			-57.5	-8.83							0.6	0.02
	NHJ-1-2	-57.6	-9.05	13.65			-57.7	-9.39							0.1	0.17
Mountain	SDJ-1			15.39*			-52.7	-7.17			-49.9	-6.71			1.4	0.23
	Recent snow	-56.0	-10.86	19.15												
				16.11*									-59.4	-8.37		

bd-denotes below detection; Std-Standard deviation of monthly data; *Sampling time in October and December rather than April.

268

Table 3 ^{222}Rn and helium isotopic data of groundwater

Sam. No.	^{222}Rn(Bq/m^3)	He content (×10^{-6})	^{4}He/^{20}Ne	^{3}He/^{4}He (×10^{-6})	R/Ra
NK8	5217				
ZK06	1182	0.8	0.29	1.92	1.37
ZK05		0.7	0.29	1.83	1.30
ZK04		4.9	0.32	1.60	1.15
ZK03	18400				
NK10	14500				
ZK01	97.00	5.3	0.39	4.90	3.50
NK1	97.00				
NK9	631.0				
NK3-1	4887				
NK3-2□	18000				
ZK09	2230				
NK13	49.00				

3. Results

3.1. Variability of stable H and O isotopes of groundwater

Monthly monitoring data show that temporal variations in δD and δ^{18}O values can be identified for most groundwater samples, while some of them even show large fluctuations (Fig. 3-5). A sine curve-like seasonal variation trend of δ^{18}O values for most groundwater samples can be identified (Fig. 4a), which the ^{18}O isotopes are distinctly depleted in April, September and December while enriched in July (Some of them also in June) and October. Some groundwater samples collected from shallow wells near the northern edge of the AFF or springs plot along the evaporation line in diagram of δD and δ^{18}O relationship that can be attributed to evaporation (Fig. 3 b and d). In contrast, the water table more than 10m below the surface, e.g. in the central part of the AFF (Table 1), evaporation effects of water in the aquifers are weak or absent. As a whole, there is a smaller change in δD and δ^{18}O for groundwater except for some groundwater samples show slightly positive shift particularly in δ^{18}O values. However, a distinctly positively shift for river water between April and June can be identified (Fig. 3a and Fig. 4a). With respect to April and June, the stable H and O isotopes of the most groundwater samples change to enriched and some of them relatively depleted in July, which is particularly maxima in samples collected from the northern edge of the AFF or springs and plot along the evaporation line with a small slope (Fig. 3c). However, the isotopes in river water also shows a smaller enriched variation in July with respect to June but they do not plot along evaporation line and locate left-upper area. Groundwater samples from some wells (ZK01,

291   ZK03, ZK04 and ZK09) in southern section and river water samples show more depleted isotopes

292   in September after summer recharge than that in previous month in July (Fig. 3b). It seems to be

293   followed by a return to high values in δD and δ^{18}O for most groundwater samples but more depleted

294   values for river water samples can be observed in October (Fig 3d). All in all, values of δD and δ^{18}O

295   in groundwater are in most cases higher than corresponding April and December values and most

296   of them show a co-fluctuation in amplitude range with groundwater table (Fig. 4b). The most

297   groundwater tables show small variations from April to June and distinctly rise to reach highest in

298   September or October. The stable H and O isotopes of the most groundwater samples also

299   correspondingly show large temporal variations after June and the largest variations can be observed

300   in July, September, and October. The groundwater table as well as δ^{18}O values return to basic level

301   as that of in April in December.

302
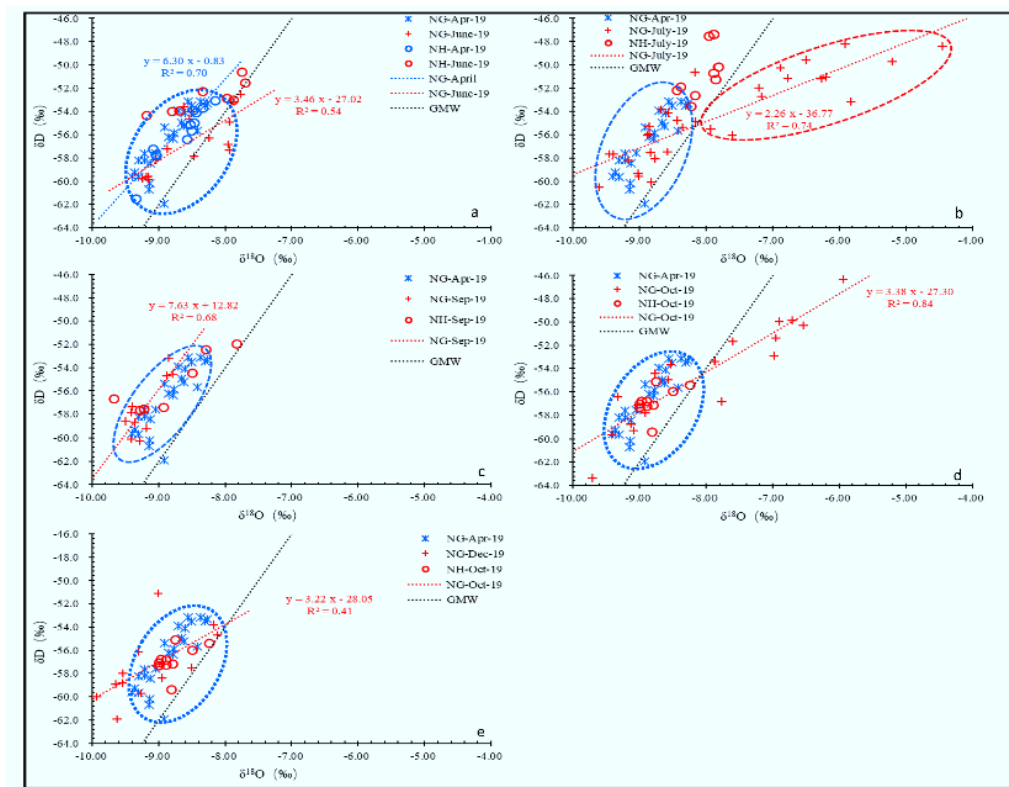
Figure 3 Diagram of the δD versus δ ^{18} O of the groundwater and river water in different months in

2019. a-June with respect to April; b-July with respect to April; c-September with respect to April;

d-October with respect to April; e-December with respect to April (No river water sample is

available due to freezing in December).

307
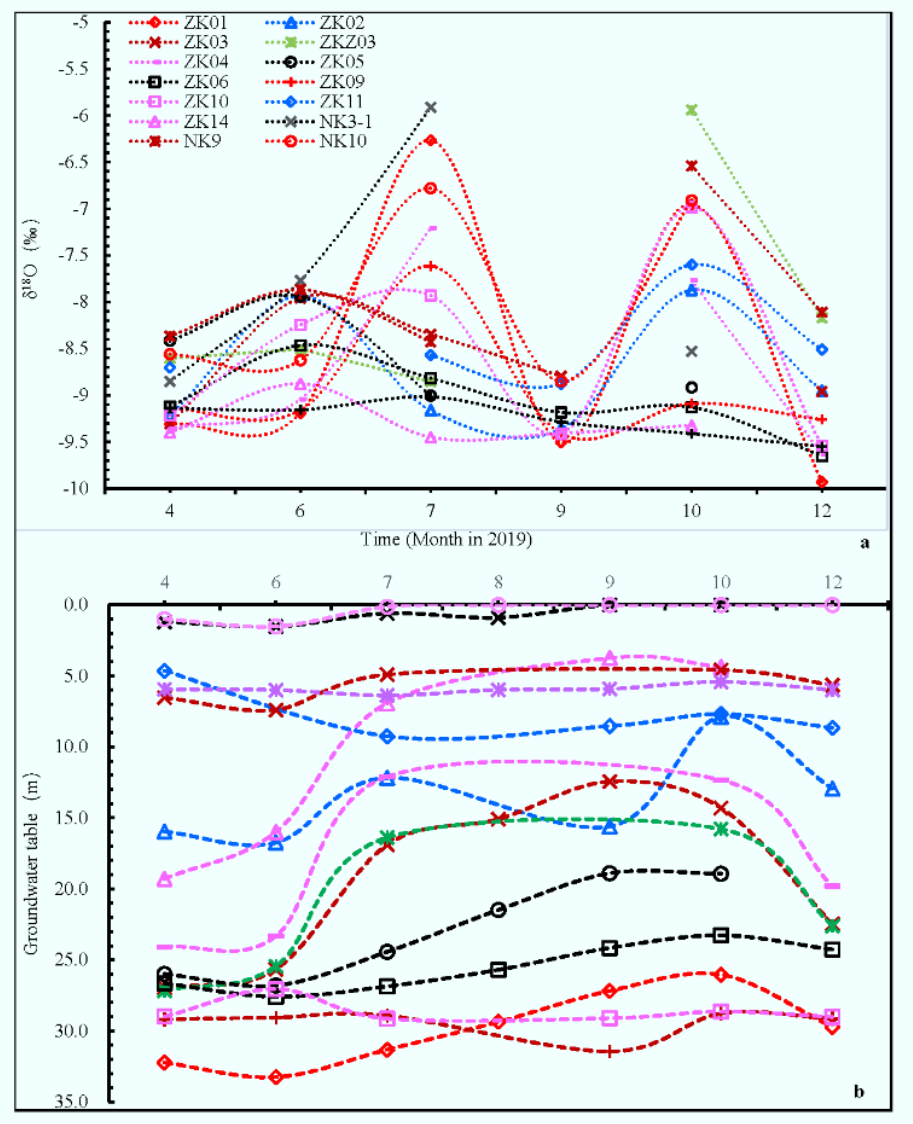
Figure 4 Seasonal (Monthly) variation of (a) stable O isotopes of groundwater and (b) groundwater table fluctuations

308

309

310

311

312

313

314

315

316

317

318

319

320

321

322

323

324
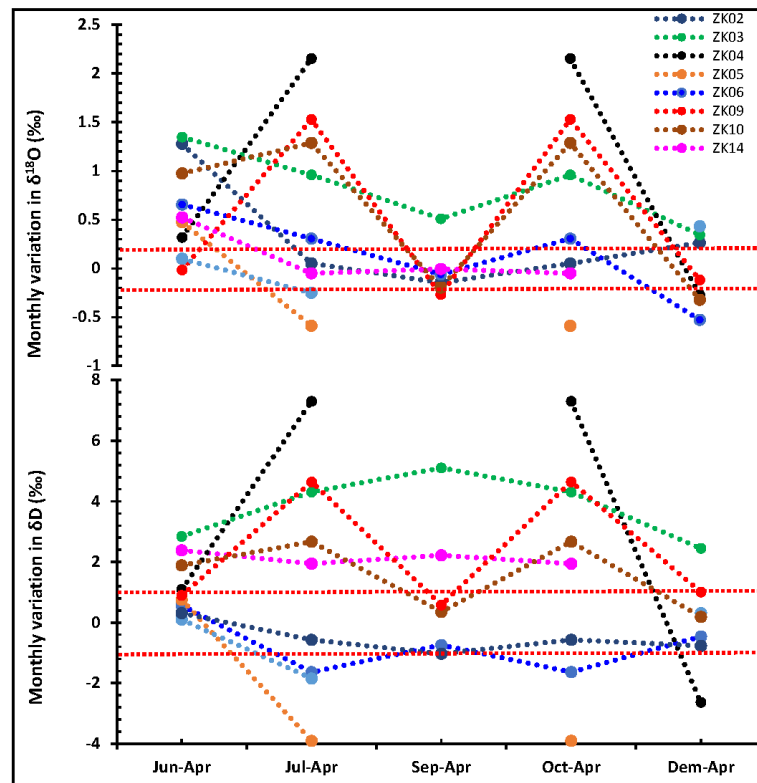
Figure 5 Monthly difference of stable H and O isotopes of groundwater. The δD and δ^{18}O values of later months (June, July, September, October and December) minus the values of April (values of base conditions). Here, the difference was selectively diagramed only for the samples with deeply buried groundwater table and distinctly monthly variations of stable isotopes. The area confined between two red dot lines denotes maximum analytical uncertainty.

330

From yearly variation for obtained data, groundwater samples from most wells show distinctly enriched variation trend in D and ^{18}O values from July 2012 to the same time in 2019 except for only two wells of ZK05 and NK3 (depleted). It seems that roughly similar variation trends of slopes about 2.0 from July 2012 to July 2019 for most groundwater samples can be observed in the diagram of δ^{18}O and δD (Fig. 6). The isotopic enrichment trend is corresponding to groundwater table rising except for well ZK04. The groundwater table in the well ZK01 has risen about 28m from July 2012 to July 2019. Correspondingly, the stable H and O isotopes show greatly enriched shifts from -8.83‰ to -6.27‰ in δ^{18}O and from -57.8‰ to -51.2‰ in δD. The large groundwater table fluctuations associated with distinct stable isotopic variations in the annual-scale can be also observed in the AFF of NR catchment.

341
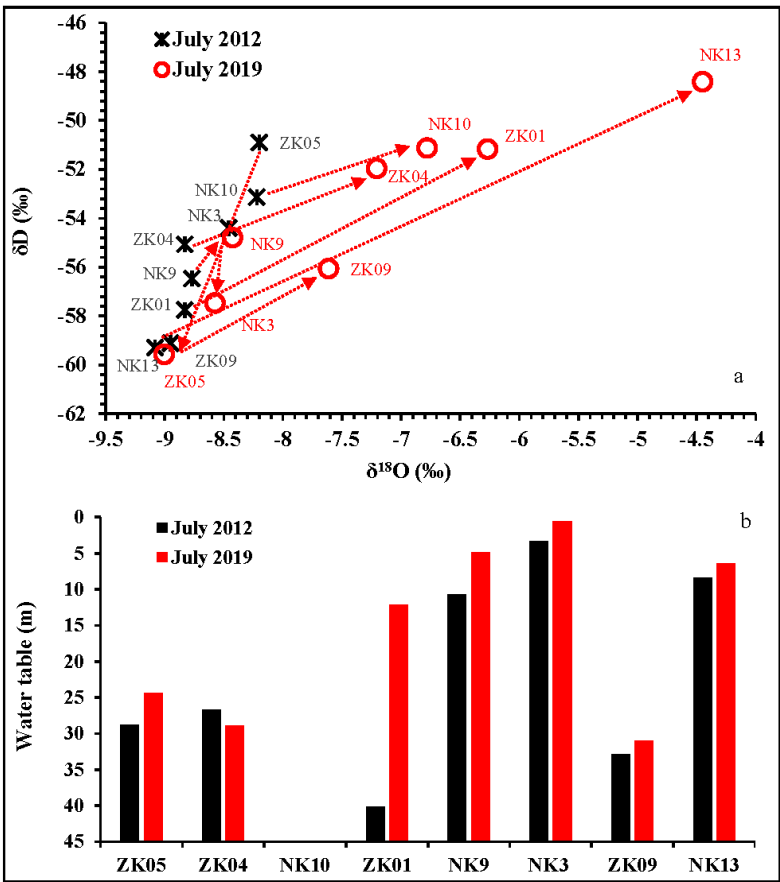
Figure 6 The variation trend of stable H and O isotopes and groundwater table fluctuation of wells between in July 2012 and 2019. From the diagram, the most groundwater tables show a rising trend while stable isotopes positive shift.

3.2. Distribution characteristics of other isotopes (T, He and ^{222}Rn) of groundwater in dry season

Almost all groundwater samples in the AFF of NR catchment show high content of tritium except for one sample from confined artesian well in the foreland nearby the fluvial plateau (CHWSQ-1 in Table 2). The T content in groundwater ranges from 7. 5TU to 19.1TU. Samples from river water show higher T content with smaller variations (15.3-17.7TU) and are similar to recent snow samples (16.11 to 19.15TU). There are no previous T data available for the NR catchment, but are similar to high tritium values reported in the neighboring Golmud River water, groundwater and precipitation if they are corrected by 28 years radio-active decay (Sun et al., 1991). The tritium content in groundwater or river water in the NR catchment is higher than that of modern

precipitation elsewhere in the northern hemisphere, where the tritium content varies between 5 and 12 TU (Morgenstern et al., 2010; Chae et al., 2019), but is close to the range of precipitation monitored in the northeastern Tarim Basin (Zhao et al., 2019) and is also close to the most recent measurements reported by the IAEA for Zhangye and Wulumuqi at about the end of the pulse of anthropogenic tritium in western China (http://www.univie.ac.at/cartography/project/wiser/). In addition, the precipitation in Tianshan Mountains and Qilian Mountains all correspondingly show high T content (Kreutz et al., 2003; Zhao et al., 2018), which indicate the NR catchment is located a typical area with high modern background T content of precipitation. There seems to be no regular spatial variation law of T content in groundwater of NR catchment, e.g. the distance from river bed or mountains and deep or shallow groundwater.

Four typical groundwater samples (Table 3) show the similar ratios in $^4He/^{20}Ne$ but larger variations in content of He and ratio of $^3He/^4He$. the groundwater samples collected from the center of AFF (ZK01 and ZK06) show higher $^3He/^4He$ ratios. In particular, the groundwater in well ZK01 shows a very high content of He (5.3×10^{-6} v/v) as well as the highest $^3He/^4He$ ratio (3.5Ra). The $^4He/^{20}Ne$ ratio in this groundwater sample is also high. Thus, the high $^3He/^4He$ ratio should be related to the high content of ^3He rather than low content of ^4He. The other groundwater samples also have $^3He/^4He$ ratios higher than 1Ra, the atmospheric rate, which suggests addition of deep-circulating water enriched in ^3He.

The content of ^{222}Rn in the groundwater in AFF of NR catchment shows a large variation from 49 to 18400Bq/m^3. If the lowest content of 49 Bq/m^3 (well NK13) in the whole catchment is regarded as local background value of groundwater, most groundwater samples show hundreds or even thousands of times higher content than local background (Table 3). This also suggests the presence of groundwater as circulated through underlying bedrock.

4. Discussion

4.1. Temporal recharge source and renewal of groundwater system

4.1.1. The law of spatial and temporal fluctuation of the groundwater table

Different from a general arid basin, the groundwater table of thick aquifers developed in AFF of NR catchment shows significant temporal variations, both in interannual, monthly, daily and hourly time scales, respectively (Fig. 7a, b and c). There are almost no human activities to affect the groundwater system, and the water table mainly fluctuates under natural conditions. Firstly, as to

389   the interannual time scale, the groundwater table in almost all wells distinctly rises during the wet

390   season from June to September (sometimes extending into October) and then, declines again after

391   following October each year. The groundwater table increases to reach the highest in September or

392   October while it drops to the lowest in April or May with also a sine curve-like fluctuation. During

393   strong recharge seasons, the groundwater table successive rising trend can be observed on daily and

394   even hourly time-scales. The groundwater table in wells ZK01, ZK03, ZK05 and ZK06, showed a

395   distinctly rising trend from July 1st to 31st in 2019 as well as within 72 hours from July 14th to July

396   16th (Fig. 7b and c). These rising fluctuations of the groundwater table in different time-scales

397   indicate rapid water recharge processes occurring during the wet season. The groundwater table

398   fluctuates every year, but concerning previous years, the groundwater table in most wells have

399   distinctly upwelled to reach the highest level for ten years in September to October 2019. For

400   example, the groundwater tables in wells ZK03, ZK01 and ZK05 have risen each year from 2010

401   to 2013 between July and September 12.38m, 10m and 5m, respectively. Most shallow groundwater

402   levels have even reached the surface or discharge as springs in the northern edge of AFF, indicating

403   that the recharge water amount or storage of groundwater have been increasing a lot since 2013 in

404   the NR catchment. The analysis of GRACE data also concluded that water storage has distinctly

405   increased in QB in recent years (Jiao et al., 2015; Xiang et al., 2016). From the seasonal time scale

406   in 2019 (Fig. 4b), the monthly groundwater table variation is similar to previous years with a

407   distinctly rising trend in the wet season while declining in the dry season. Most wells with deeply

408   buried groundwater table in the southern monitoring section (around the centre of AFF) also show

409   distinctly rising trends after recharge since April. Groundwater tables in the well ZK14 nearby the

410   mountain front and ZK03 adjacent the mainstream rose from April to September close to and over

411   15m, respectively. The groundwater table in ZK03 and ZK01 rose within one-month over 2m and

412   over 5m, and about 0.1 to 0.5m within 72 hours in July, respectively (Fig. 7b and c). Reversely, a

413   few wells around the Hongxing Water Supply Company (No. ZK11、ZK09、NK13 and ZK10) do

414   not show a distinctly rising trend of the groundwater table in summer and even some decline, which

415   should be related with increasing anthropogenic freshwater extraction counterbalancing the natural

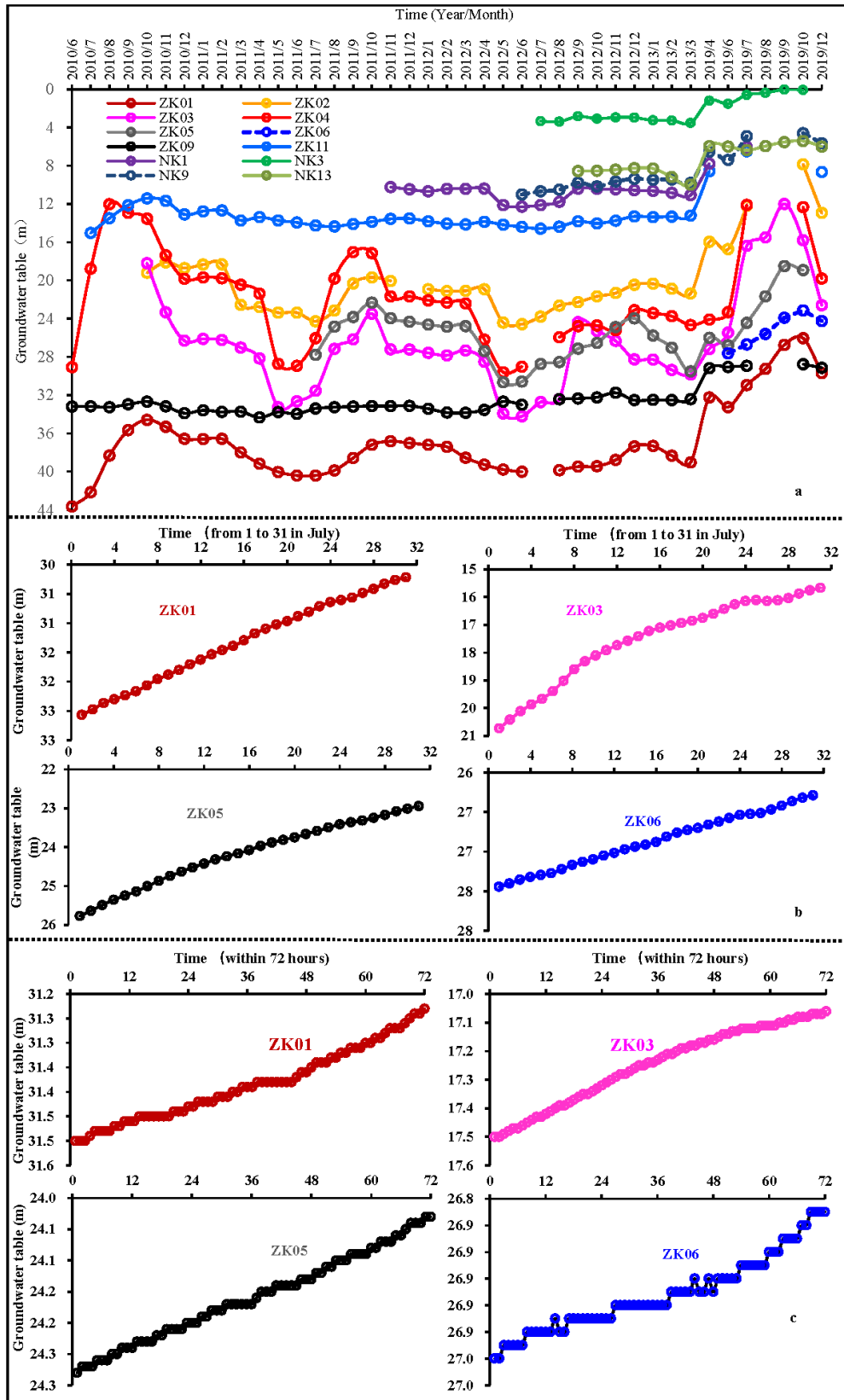416   rising trend on a local scale.

417

418

419 **Figure 7** Groundwater table fluctuations in the time-scale of (a) year/month, (b) day/month and (c)

420 hour/day in the AFF of NR catchment (Data within 72 hours recorded from 14 to July 16th 2019

421 using high-precision automatic water gauge (HOBO U20 Ti).

422　　　From the spatial variations of groundwater table, the wells with more significant dynamic

423　　fluctuations mainly distribute around southern monitoring section and close to mountains, where

424　　the well ZK14 nearby the mountain front show the most considerable monthly groundwater table

425　　difference. Also, the wells ZK03, ZK04 and ZKZ03 located nearby and ZK05 or ZK06 far away

426　　from the mainstream show a more substantial groundwater table fluctuation of a rising trend after

427　　April. The monthly fluctuation of groundwater table becomes smaller and smaller from the

428　　mountains to the northern edge of the AFF, which is corresponding to a general catchment. However,

429　　the different characteristic from a general mountain-river-basin system is that groundwater table

430　　fluctuation seems to be no natural law with the distance from the mainstream. Generally, the closer

431　　to the mainstream is, the more substantial variation of groundwater table occurs for river water

432　　regularly infiltrates to recharge groundwater when flows across the AFF. That is, the groundwater

433　　table will relatively maintain stable due to the slower recharge and longer renewal time if it is far

434　　away from the mainstream or river channels. However, there seem to be no corresponding tight

435　　relationships between groundwater dynamics and distance to the significant river channel in AFF

436　　of NR catchment. This unusual scenario is related to individual preferential conduits for

437　　groundwater recharge through faults or other structures in the mountains rather than only dependent

438　　on river water infiltrating through unsaturated zones in the basin. The mechanism will be discussed

439　　in later sections.

440　　　At present, the groundwater dynamics are mainly governed by a natural recharge and discharge

441　　balance in the NR catchment. The distinctly rising groundwater table during the wet season in the

442　　thick aquifers in the centre of the AFF (with water table buried over 10m or 20m, respectively)

443　　indicates favourable circulation conditions of the groundwater system and bears great significance

444　　for water resources exploration in the future. Moreover, the interannual groundwater table

445　　fluctuation law in the NR catchment is not only the response for seasonal climate changes every

446　　year but also as a response to constant climate warming in the last ten years.

447

448　　**4.1.2. Water source inferred from temporal variability of stable H and O isotopes**

449　　　Previous results show that the stable H and O isotopes in groundwater for most wells in the

450　　AFF of the NR catchment display distinct or identified temporal variations, particularly seasonal

451　　effects also display sine-like curves corresponding to groundwater table fluctuations (Fig. 4 and 5).

452　　Thus, the rising groundwater table and corresponding variations in stable isotope records during the

453   wet season argues for water recharge and at least partly renewal of old water in the aquifers. Some

454   groundwater samples from wells or springs located near the northern edge of the AFF display

455   different intensities of evaporation effects for the shallow groundwater table and δD and $\delta^{18}O$

456   obtained within plot along the evaporation line (see Fig. 3 b, d). Groundwater samples from wells

457   in the centre of the AFF and nearby the mountain front plot in the upper-left area of the global

458   meteoric water line (GMWL), arguing for a local continental derived source. This scenario is

459   widespread in the groundwater circulation system in the high-cold Tibetan Plateau (Li et al., 2020).

460   Kong et al. (2019) concluded that non-monsoon precipitation, sourced from inland glaciers on the

461   Tibetan Plateau, govern the groundwater recharge in the foreland basin, where the local monsoon

462   precipitation, sourced from the ocean, plays negligible effects. The groundwater recharge in the

463   exceptionally arid QB basin should further follow this trend as it receives only scarce precipitation.

464   The primary recharge source therefore originates from precipitation of local moisture circulation

465   patterns in the high elevation of the eastern KM, where waters can directly infiltrate and recharge

466   the groundwater and rivers.

467   In the dry season in April, the groundwater table drops to reach the lowest state and stable H

468   and O isotope compositions in the groundwaters are relatively lighter (than values obtained later in

469   the year) and plot close to river isotopic compositions. Consequently, both the river and groundwater,

470   reveal similar a source, i.e. the discharge of groundwater in the mountains as the base flow of the

471   NR. During winter in the permafrost region, nearly the entire river base flow is contributed by

472   groundwater discharge (Liu et al., 2012). Until June, the glacial-snow meltwater shows greatly

473   increasing trends, however, significant precipitation does not occur. Following Sergey et al. (2009)

474   snow sublimation causes kinetic isotope fractionation leading to an enrichment in heavy H and O

475   isotopes in the meltwaters. Consequently, the H and O isotope compositions of rivers fed by

476   meltwaters should become isotopically heavier than that in April. However, the isotope

477   compositions in groundwater in AFF show no significant variations between April and June, despite

478   the groundwater table rising (Fig. 3a). This suggests that the proportion of new recharge water in

479   the aquifers may be too small for significant impact on the isotopic compositions, or new recharged

480   water hasn't reached the aquifers in the AFF within two months' lag time. From July, temporal

481   precipitation occurs occasionally, while the glacial meltwater flux increases to its largest level and

482   evaporation is the strongest. For wells or springs near the northern edge of the AFF, evaporation

483   causes H and O isotope fractionation towards heavier values recorded in the groundwater (Fig. 3b).

484   Most groundwater samples plot along the evaporation line with a good linear relationship (R^2=0.74).

485   The negative end-member is defined by groundwater samples from the centre and the southern area

486   of the AFF. A trend line fitted through samples from near the northern edge of the AFF reversely

487   extends to the left-lower corner, which means that the groundwater developed in the centre and

488   southern area, as well as the northern edge of the AFF, have a similar source. The groundwater

489   flows from the center to the northern AFF and surface discharge as springs and in swamps or

490   wetlands. Thus, here it only needs to trace the source of groundwater in the centre of AFF for weak

491   or negligible evaporation effects on stable isotopes. Concerning April, the distinct enriched shift in

492   stable H and O isotopes in the groundwater and river, as well as rising water table in the AFF in

493   July (Fig. 4), suggest juvenile water input into the aquifers. The new water should originate from

494   upper reaches of the NR with heavier isotopes (sample No. NH7 and NH8) as well as meltwater

495   from high elevation vertical infiltration. The groundwater table gradually rises to reach the highest

496   level in September and October after successive recharge during the wet season (Fig.7). The rising

497   groundwater table makes the most areas become a swamp in the northern edge of the AFF making

498   the research area inaccessible from September on. According to recent three years' monitoring data

499   in the source region of the Yangtze River (Li et al., 2020), the precipitation dominates and accounts

500   for 48% of runoff with the maximum temperature and precipitation occurring and stable H and O

501   isotope compositions changing to lighter values in August. The climate is similar in the source area

502   of the NR with the source region of the Yangtze River. So, although there is no precipitation sample

503   available, the distinctly depleted H and O isotopes in the groundwater in September in the AFF of

504   NR catchment should be more likely caused by replenishment of mountain precipitation from July

505   to September. Compared to April, the groundwater in October exhibits distinctly heavier H and O

506   isotope compositions (Fig. 3c). In particular, the groundwater samples from the northern edge of

507   AFF in October also show distinct evaporation effects in H and O isotopes and samples plot along

508   the evaporation line with an obvious linear relationship (R^2=0.84) (Fig. 3d). The negative end-

509   member of reversely extensive evaporation line is also very close to samples from the centre of the

510   AFF. Considering the rising by a wide margin of groundwater table in September and October, the

511   successive recharge since July correlates to a response at the end of the wet season. The stable H

512   and O isotopes in groundwater in the centre AFF changes to relatively enriched and is closer to river

513   water. In contrast, the groundwater table gradually drops after October. The reason why the

514   groundwater table naturally declines and gradually recovers to its base condition is mainly attributed

to a large water discharge at springs in the edge of the AFF as well as laterally runoffs into the northern lakes, indicating that the groundwater system fully adjusts after the strong recharge during the wet season. The stable H and O isotopes of groundwater in December return to base values like in April with recharge source water changes to base flow (mainly fed by spring water) in the mountains.

Due to the very complicate nature of water source compositions and seasonal variations in a high-altitude cold-climate mountains and basin system, it's hard to estimate the large seasonal proportion of groundwater accurately. Here, some typical wells with deep groundwater table (>20m) and sizeable seasonal water table fluctuations (>5m), as well as identified seasonal variation of stable isotope compositions, were selected to statistically estimate the recharge proportion of the groundwater system during the wet season from June to September. The groundwater in June can represent the beginning of large-scale recharge. The groundwater in September can be regarded as a mixture of new and old water after substantial recharge. Then, the recharge proportions of groundwater can be estimated using the isotope mass balance equation:

$$f \times \delta^{18}O_r + (1-f) \times \delta^{18}O_g = \delta^{18}O_m$$

where $\delta^{18}O_r$ denotes for the isotopic composition value of the main recharge source water during the time from June to September (-9.47‰, average river value of the upper NR before flowing out the mountains in September). $\delta^{18}O_g$ denotes for the old groundwater isotopic end-member contained in the aquifers in June (-8.58‰, averaging data for groundwater of wells with table rising over 5m in the centre of the AFF), $\delta^{18}O_m$ denotes for the isotopic composition of the mixture of groundwater in September (-9.24‰, averaging data for groundwater of the same wells as in June), and f indicates the mixing proportion (%). The calculation results show that the river water proportion in the mix is in the order of 68% while old water accounts for the remaining 32%. Therefore, 68% groundwater was replenished during the wet season from June to September in 2019 for groundwater samples with large water table fluctuations in the centre of the AFF of the NR catchment. It is that large proportion of new water added in the aquifers that drives the groundwater table to rise up to 15m

541   after recharge during the wet season.

542

4.1.3. Replenished period and estimated age of groundwater inferred from isotopes and water table

Almost all wells show high contents of T in the groundwater except for one confined groundwater sample collected in the northern edge of the AFF of the NR (Table 2). The T content in most groundwater samples matches river concentrations. Two typical wells (ZK10-11) with the highest T content have very rich groundwater with water yields of more than 5000m^3/d (data from the pumping test), denoting for excellent circulation conditions in the groundwater system. There has been no T released by new atmospheric thermal nuclear tests since the Comprehensive Nuclear Test Ban Treaty in the 1990s. All the river water samples in the NR show higher T content than 15TU and are close to recent snow meltwater concentrations of 19.15TU (Fig. 8), suggesting that the river water even at base flow state in April mainly originates from current precipitation. The T content in the adjacent Golmud River ranged from 84 to 123TU in 1987 and from 42.6 to 67.0TU during rainfall in 1998 (Sun et al., 1991). All these datasets exhibit a distinct higher background T content. According to the radioactive decay law, current precipitation should have T contents ranging from 14 to 21.96TU, which overlaps with recent snow meltwater concentrations (19.15TU). The T content is also close to concentrations obtained during a precipitation event in 1998 if it is assumed that the river water in 1987 can represent the current meteoric water and further experienced about ten years' of radioactive decay. All these facts approve that the T content in the river water can roughly describe the background value of the current precipitation. So, the groundwater samples with high T content (closing to content of river water) should be recently recharged and the renewal period may probably be limited within yearly or even seasonal time scale (Fig.8). In contrast, the groundwater sample with the second-highest T content (10-15TU) mean that relatively older water, recharged several years ago, likely occupies a more substantial proportion. The circulation period should be within 0 to 12 years with less than a half-life of tritium. The very young groundwaters with higher T contents (over 10TU) are mostly located in the centre or southern area of the AFF. In addition to higher T content, the circulation period for other groundwater samples with relatively general T content (5-10TU) may be probably recharged over ten years but less than two half-lives (within 24 years) or even older. There seems to be no natural variation law of groundwater replenished period in the the AFF except for a very young age in the mountains and

572   relatively older age in the alluvial plains. Almost all groundwaters developed in thick aquifers of

573   the AFF in the the NR catchment (over 150m or 250m in depth) should be very young and can be

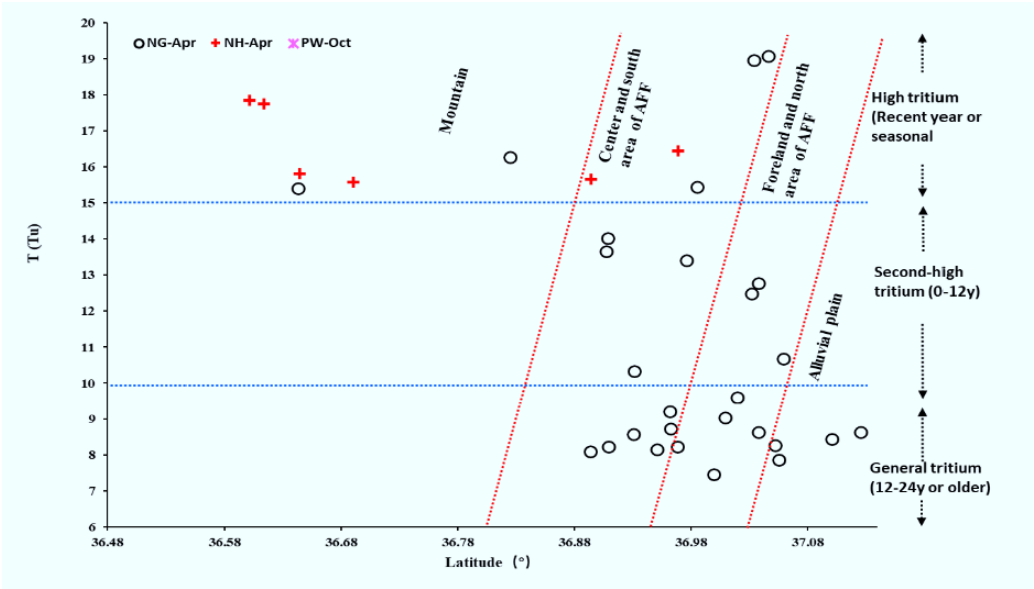574   classified as a modern groundwater circulation system.

575

576

Figure 8 Estimated replenished period of groundwater systems from Mountains to Basin in the
Nalenggele River catchment (NG-Apr denotes samples of groundwater in April; NH-Apt denotes
samples of the river in April; PW-denotes snow samples collected from mountains in October)

580

4.2. Conceptual model of the hydrological processes controlling rapid groundwater circulation

system

Generally, river water can infiltrate to recharge groundwater through loose alluvial or fluvial

deposits when it flows out of mountains into the basin. However, there is no adequate river water to

recharge groundwater and to account for a groundwater tables' monthly rise by several meters or

decameters. Over 70% of the NR water is lost in the mountains, and it is almost completely

evaporated after flowing out of the mountains during the dry season. Besides, it should be a long

time only dependent on water to infiltrate through thick vadose to recharge groundwater. Thus, there

might be a mechanism governing the rapid recharge and circulation of groundwater forming

abundant groundwater resources in the the AFF of the NR catchment.

As an area with intense tectonic and volcanic activities in the mountains as well as a very young

groundwater system with rapid recharge and circulation in the AFF of the NR catchment, the

unusual high $^3He/^4He$ ratios in the groundwater are more likely related to deep fluids or upwelling

mantle de-gassing. Previous studies concluded that the formation of unique salt-lake resources with extreme enrichments in B, Li and other incompatible elements as well as high concentrations both in rivers and groundwater in the NR catchment might be mainly sourced from deep fluids (Tan et al., 2012). The high content of ^{222}Rn in the groundwater further indicates the development of faults or other large-scale fractures effecting the groundwater circulation system. The groundwater in some wells in the centre of the AFF of the NR shows a large groundwater table rising trend in the wet season as well as distinct stable H and O isotopic variations and high content of T. All these characteristics correspondingly suggest favorable structures as conduits developed for groundwater rapid recharge and circulation.

Generally, water flow in crystalline basements is enabled by the occurrence of interconnected fracture networks (Bucher and Stober, 2010) and the presence of hydrological driving forces (Ingebritsen and Manning, 1999). Mountain topography has been long ago recognized as a critical driver for precipitation deep and long-distance circulation. The tectonic, topography and geomorphological characteristics are special in the upper or source area of the NR, which are very different from the general river catchment. As a centre of collision and convergence of the Altyn Mountains and the Kunlun Mountains, a series of deep and large-scale faults and many kinds of volcanic craters have been developed (Fig. 2). Besides, recent intense tectonic activities, the Kunlun Mountains are still rising, while the QB is relatively declining (Wang et al., 2012; Zhou et al., 2018). A massive earthquake (Ms 8.1) happened on November 14th 2001 along the NWW slip fault belonging to the eastern Kunlun fault zone. Geological investigations found that a 350km-long left-lateral rupture zone with a maximum left-lateral displacement over 6m have been developed since the earthquake (Yin et al.，2002). Klinger et al. (2005) concluded that the earthquake ruptured a 450-km-long stretch of the sinistral Kunlun strike-slip fault, at the northeastern edge of the Tibet plateau. These young (Quaternary) deep faults cut through the source area of the branch of HR catchment, which has developed very significant hydrothermal activity and deep fluid circulation (Tan et al., 2012). Moreover, frequently occurring volcanic activity developed many kinds of craters in ancient times, with the latest eruptions in 1952 and 1984 in the source area of the NR (Zhu, 1989). Thus, the favorable conduits have been developed in the source area and the upper NR (including HR and CR branches) under the background of these tectonic and volcanic activities (Fig. 9). The high content of ^{222}Rn and ^{3}He/^{4}He ratios indicate deep fluids or gas can move upward to reach the shallow aquifers. These profound substances can generally move upward along deep faults. Thus, a

625   unique condition of groundwater circulation system in the NR catchment is that, in addition to

626   general conduits for shallow groundwater circulation, the active significant faults or craters can be

627   well acted as favorable conduits for deep groundwater circulation. This is furtherly certified by

628   considerable enrichment of elements of B and Li (over ten times higher than general freshwater) in

629   the very fresh groundwater as well as large-scale B and Li resources developed in the tail salt lakes

630   (Tan et al., 2012).

631

632
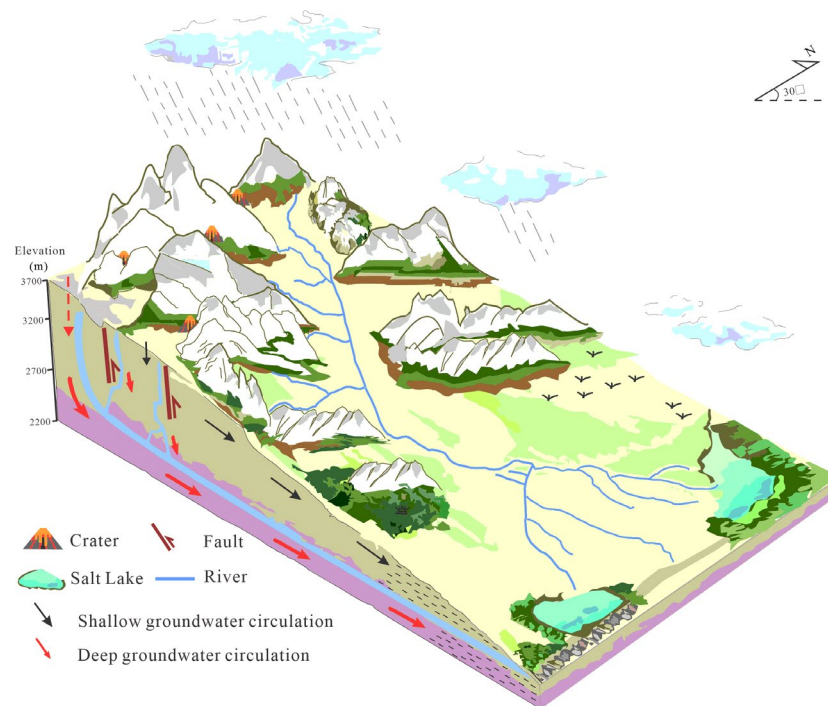
633   **Figure 9** Conceptual model indicating the rapid groundwater circulation process in a typical high-
634   cold mountain-arid basin system

635

636   In addition to excellent conduits for groundwater recharge and runoff, the plentiful water

637   sources and large water head fall from source to aquifers in the AFF of NR catchment are also an

638   essential critical condition to drive rapid surface water to groundwater recharge and underground

639   circulation. Large-scale glacial and snow cover the northern slope of the eastern KM where

640   abundant summer precipitation occurs as well. The steady flow of glacial-snow meltwater and

641   temporal precipitation supply are an adequate water source both for the NR and groundwater. In

642   particular, the elevation in the source area of the high mountains is over 4000-5000m a.s.l. while it

643   declines to lower than 2900m in the principal aquifers of the AFF of the NR. Thus, these abundant

644   source waters in the high mountains can vertically and rapidly infiltrate along favorable conduits

645 (significant faults and crater) and then laterally move along all kinds of structures including shallow

646 pores within loose sand-gravel deposits to recharge groundwater in the AFF under over 1000-2000m

647 water head fall. Overall, the abundant water source yielded in high mountains, favorable conduits

648 of significant faults and craters in the mountains and macropores developed in shallow sands or

649 gravel strata in the middle-lower reaches. Excellent water head difference from the source area of

650 high mountains to aquifers in the lower basin combinedly drive and maintain the rapid recharge and

651 circulation processes of groundwater all the round between high-cold mountains and low basin

652 system. As for such abundant groundwater resources developed in the AFF of NR catchment, in

653 addition to above preconditions, it is also related to very thick aquifers over 100m to 200m with

654 sands-gravel deposits, which supply adequate space for groundwater storage.

655 Based on the rough water budget, local hydrological observations conclude that enormous

656 quantities of groundwater resources have developed in intermontane basins of upper-middle reaches

657 of the NR catchment for over 70 percent of the river water infiltrated to recharge groundwater before

658 the river flowing out of the mountains (Wang et al., 2008). The conceptual model of the hydrological

659 processes of groundwater circulation between the mountains and basin in the NR catchment issued

660 in this study furtherly believes it a reasonable presumption. Moreover, it seems to be much likely

661 that there have collections between groundwater system in intermontane basins at higher elevation

662 and groundwater in QB at lower elevation through underground conduits.

663

664 **4.3. Trend prediction on groundwater table fluctuation and storage**

665 Many previous studies approved that the climate warming is very distinct on the Tibetean

666 Plateau and the QB is one of the areas with the most substantial temperature rise (Jiao et al., 2015;

667 Xiang et al., 2016; Kuang et al., 2016). From the meteorological records (since 1956) of trendline

668 of annual temperature and total precipitation variations in Golmud station nearby research area (Fig.

669 10), the precipitation displays large-scale fluctuations for different years, and the fitted linear

670 trendline is not very distinct (R^2=0.14). A weak, increasing trend of rainfall since 1956 can be

671 identified. In contrast, a very definite rising trend of temperature with an excellent linear correlation

672 (R^2=0.85) can be observed. The average rise in temperature is in the order of 0.06℃/year over the

673 past 60 years. The temperature has never dropped to be lower than 4℃ since 1970 and maintained

674 over 6℃ in the recent 20 years. Successive warm climate might be expected to accelerate the

675 shrinkage of glaciers and permafrost and increase the availability of water in the source or upper

676 NR catchment. The more enriched in stable H and O isotopes in the groundwater as well as water

677 table rising in July 2019 than that the same time and same well in 2012 in the AFF of NR catchment

678 may be more likely related to the response of this hydrological process (Fig. 6). The response

679 mechanism governing the distinctly enriched stable H and O isotopic variation in groundwater needs

680 furtherly to be tracked. It possibly indicates that the recharge water proportion from glacial melting

681 of permafrost releasing increases under the effect of climate warming. The evaporation and

682 sublimation processes in snow, ice and permafrost samples shows significant fractionation in

683 observed $\delta^{18}O$ and δD in residual meltwater (Sergey et al., 2009). This means that the proportion

684 of meltwater from remaining snow or ice and permafrost releasing water after a long time of

685 evaporation (and associated sublimation) increases in the groundwater for successive climate

686 warming from 2012 to 2019. Besides, the precipitation will also increase in the high mountains with

687 temperatures rising in the area. For example, in the Qilian Mountains, the contribution of recycled

688 moisture to rainfall increased by 60% since 1990, which has increased runoff and changed seasonal

689 runoff patterns and runoff components (Li et al., 2020). Thus, the total water in the recharge area

690 will increase significantly with glacial-snow-permafrost meltwater and temporal precipitation

691 increasing.

692
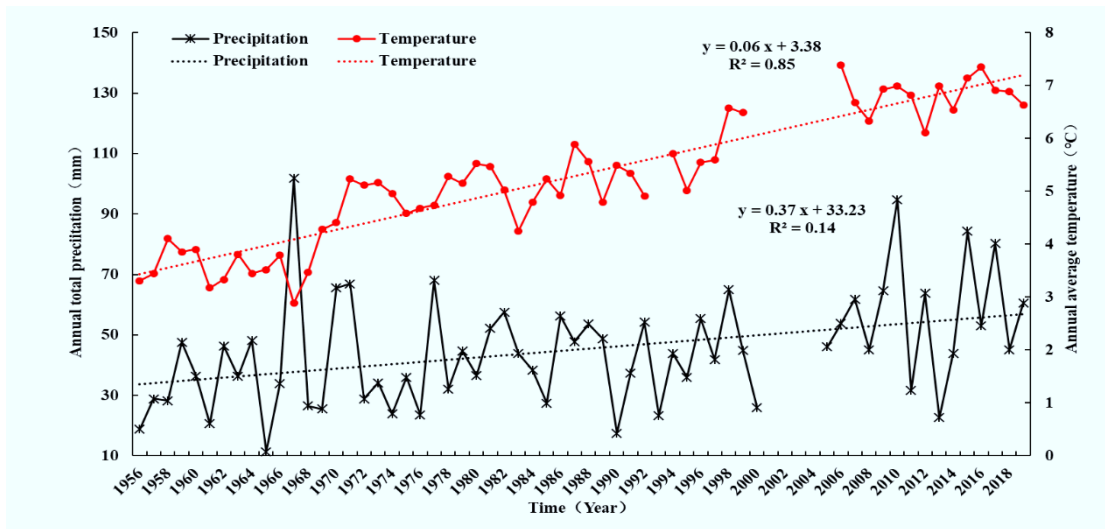
693 **Figure 10** Meteorological records (trendline of annual temperature and total precipitation variations)

694 from Golmud station nearby Nalenggele River catchment.

695

696   Although there are no long-term monitoring records in the mountains for hard natural

697 conditions, sporadic monitoring data found that over 70 per cent of the river water infiltrated to

698 recharge groundwater before the river flowing out of the mountains (Wang et al., 2008). Field

699 observation of this study in 2019 also noticed that the runoff of two upper main branches of CR and

700 HR had a substantial quantity of water at the end of spring and summer. Still, most of the water lost

701 after flowing out the mouth of mountains and the river was almost dried up in the basin. This means

702 that the groundwater in the AFF of NR catchment mainly receives recharge from lost surface water

703 in the mountains rather than the recharge from river runoff in the basin. Thus, it can be well predicted

704 that the groundwater table will substantially rise if the total water in the mountains (recharge area)

705 increases with the successive climate warming expected in the future. Moreover, a large reservoir

706 has been building in the NR at the mouth of mountains in future ten years. The rising trend of

707 groundwater table will be more accelerated for the recharge water will increase driven by the

708 hydraulic pressure increasing when much more water is retained in the reservoir. The rising

709 groundwater table will increase the water storage and yield more water resources for the QB while

710 it will also result in potential natural hazards. The substantial rising groundwater table will easily

711 incur serious salinization and alkalinization in the extremely arid basin. Besides, the oasis located

712 in the northern edge of AFF will much likely be perennially submerged into water and lose the

713 natural ecological function due to much more water discharged under groundwater table rising. The

714 tail Salt Lake resources (K, B and Li minerals) will also be affected by increasing discharge water.

715 Therefore, the exploration of water resources in the NR catchment cannot only become dependent

716 on surface water in the future with facing climate changes. The exceptionally rapid groundwater

717 circulation characteristic between the high-cold mountains and arid basin system impels the

718 practicable development of superior groundwater resources. The development and utilization of rich

719 and excellent groundwater resources in the AFF of NR catchment must control a reasonable scale,

720 which can abstract water to satisfy other town or cities with water resources scarce but large-scale

721 demands, such as adjacent Golmud city and northern QB, and while must maintain groundwater

722 table fluctuates in a balance or reasonable dynamic state and prevent it from over rising.

723

5. Conclusions

725   1) A distinct seasonal or monthly fluctuation of groundwater table as well as identified stable

726 isotopic variations can be observed in the AFF of Nalenggele River catchment in Qaidam Basin.

727 The large-scale rising groundwater table with identified stable isotopic variations during the wet

728 season indicate the large proportion of seasonal renewal of groundwater occurring. The recharge

source of groundwater in the fan mainly originates from surface water vertical infiltration in the Kunlun Mountains.

2) Both the river and groundwater have a high concentration of radio tritium, which the content is very close to current precipitation. Combining high content T with the association of significant seasonal groundwater table dynamics and stable isotopic seasonal effects, the age and renewal rate of groundwater should be very rapid. The groundwater seems to be very young with recharge age about 0-12 years for aquifers developed in the centre and near the mountain front or mountains and about 12 to 24 years in the northern edge of the AFF of NR catchment. Some confined groundwaters with almost free T content in the alluvial-fluvial plateau may be over 60 years before recharge and need to be furtherly approved.

3) The mechanism governing the formation of abundant groundwater and rapid circulation in the AFF in extremely arid Qaidam Basin may be mainly related to several favorable hydrological conditions. Firstly, the plentiful water from glacial-snow melt and temporal precipitation in the high mountains supply adequate recharge source. Secondly, large-scale active faults and volcanic craters and other macro-structures can be acted as favorable conduits to drive abundant source water to infiltrate and laterally runoff vertically. Thirdly, the massive hydraulic head, over 1000-2000 m, appears to rapidly drive infiltrated water flow over distances from recharge area in high mountains to the alluvial-fluvial fan. Finally, the very thick loose sands and gravel strata over 100 or 200 m supplies enough groundwater storage space in the basin. Thus, the rapid groundwater circulation system and affluent groundwater resources can also be developed even in the very arid basin far away from the recharge area.

4) The successive warm climate in the future might be expected to accelerate the shrinkage of glacial and increase precipitation in the high Kunlun Mountains. As a response, the trend of groundwater table in the AFF of NR catchment will rise more rapidly and dramatically with recharge water increasing in the source area. Thus, it will supply more superior water resources for arid Qaidam Basin as well as prevent oasis and soil from salinizing and alkalinizing if groundwater in the alluvial-fluvial fan is reasonably explored in the future.

References

Aude, V., Sophie, V., & Guðfinna, A. (2019). Groundwater in catchments headed by temperate glaciers: A review. Earth-Science Reviews 188, 59–76. https://doi.org/10.1016/j.earscirev.2018.10. 017

Bucher, K., Stober, I., (2010) Fluids in the upper continental crust. Gefluids, 10, 241–253. https://doi.org/10.1111/j.1468-8123.2010.00279.x

Bijeesh, K.V., Wang, S.S., Sergio, F. S., Ulisses, F.B., & Jefferson, C.S. (2017). Glacier monitoring and glacier-climate interactions in the tropical Andes: A review. Journal of South American Earth Sciences, 77, 218-246. https://doi.org/10.1016/j.jsames.2017.04.009

Currell, M.J., Cartwright, I., Bradley, D.C., & Han, D. (2010). Recharge history and controls on groundwater quality in the Yuncheng Basin, north China. Journal of Hydrology, 385, 216–229. https://doi.org/10.1016/j.jhydrol.2010.02.022

Clarke, I., & Fritz, P. (1997). Environmental Isotope in Hydrogeology, Springer-Verlag, Lewis Publishers, New York, https://doi.org/10.1007/s00254-002-0677-x

Chae, J.S., & Kim, G., (2019), Seasonal and spatial variations of tritium in precipitation in Northeast Asia (Korea) over the last 20 years. Journal of Hydrology, 574, 794–800. https://doi.org/10.1016/j. jhydrol.2019.04.058

Chen, Z.Y., Qi, J.X., Xu, J.M., Ye, H., & Nan, Y.J., (2003). Paleoclimatic interpretation of the past 30 ka from isotopic studies of the deep confined aquifer of the North China plain. Applied Geochemistry, 18, 997–1009. https://doi.org/10.1016/S0883-2927(02)00206-8

Chen, J.S., & Wang, C.Y. (2009). Rising springs along the Silk Road. Geology, 37, (3), 243-246. https://doi.org/10.1130/G25472A.1

Chen, H., Zhu, Q., Peng, C.H., Wu, N., Wang, Y.F., Xiu Q.F., et al. (2013). The impacts of climate change and human activities on biogeochemical cycles on the Qinghai-Tibetan Plateau, Global

Change Biol, 19(10), 2940–2955, https://doi.org/10.1111/gcb.12277

Gleeson, T., Befus, K.M., Jasechko, S., Luijendijk, E., & Cardenas, M.B. (2016). The global volume and distribution of modern groundwater. Nature Geoscience, 9, 161–167. https://doi.org/10.1038/ngeo2590

Gates, J.B., Edmunds, W.M., Darling, W.G., Ma, J., Pang, Z., & Young, A.A. (2008). Conceptual model of recharge to southeastern Badain Jaran Desert groundwater and lakes from environmental tracers. Applied Geochemistry, 23, 3519–3534. https://doi.org/10.1016/j.apgeochem.2008.07.019

Glenn, E.P., Scott, R.L., Nguyen, U. & Nagler, P.L. (2015). Wide-area ratios of evapotranspiration to precipitation in monsoon-dependent semiarid vegetation communities. Journal of Arid Environments, 117, 84-95. https://doi.org/10.1016/j.jaridenv.2015.02.010

Guo, G.D., & Wu, T.H. (2007). Responses of permafrost to climate change and their environmental significance, Qinghai-Tibet Plateau, J. Geophys. Res, 112, F02S03. https://doi.org/10.1029/2006JF000631.

Gascoyne, M., Wuschke, D.M., & Durrance, E.M. (1993). Fracture detection and groundwater flow characterization using He and Rn in soil gases, Manitoba, Canada. Applied Geochemistry, 8, 223-233. https://doi.org/10.1016/0883-2927(93)90037-H

Ge, S.M., Wu, Q.B., Lu, N., Jiang, G.L., & Ball, Li. (2008). Groundwater in the Tibet Plateau, western China. Geophysical Research Letters, 35(18), 80-86. https://doi.org/10.1029/2008GL034809

Gao, Y.H., Xia, L., Leung, L.R., Chen, D.L., & Xu, J.W. (2015). Aridity changes in the Tibetan Plateau in a warming climate. Environ. Res. Lett, 10(3), 034013. https://doi.org/10.1088/1748-9326/10/3/034013.

Hartmut, W., Hafzullah, A., Konrad, & Miegel. (2019). Fast response of groundwater to heavy rainfall. Journal of Hydrology, 571, 837–842. https://doi.org/10.1016/j.jhydrol.2019.02.037

Ingebritsen, S.E., & Manning, C.E. (1999). Geological implications of a permeability-depth curve for the continental crust. Geology, 27, 1107–1110.https://doi.org/10.1130/0091-7613(1999)0272.3.CO;2

Ji, Z., & Kang, S., (2013). Double-nested dynamical downscaling experiments over the Tibetan Plateau and their projection of climate change under two RCP scenarios. Journal of the Atmospheric Sciences, 70(4), 1278–1290. https://doi.org/10.1175/JAS-D-12-0155.1

Kendall, C., & McDonnell, J. J. (1998). Isotope Tracers in Catchment Hydrology. Elsevier.

822   https://doi.org/10.1029/99EO00193

823   Jasechko, S., Perrone, D., Befus, K.M., Cardenas, M.B., Ferguson, G., Gleeson, T., et al. (2017).

824   Global aquifers dominated by fossil groundwaters but wells vulnerable to modern contamination.

825   Nature Geoscience, 10, 425–429. https://doi.org/doi:10.1038/ngeo2943

826   Jiang, W. J., Wang, G. C., Sheng, Y, Z., Shi, Z. M., & Zhang, H. (2019). Isotopes in groundwater

827   (^{2}H, ^{18}O, ^{14}C) revealed the climate and groundwater recharge in the Northern China. Science of the

828   Total Environment, 666, 298–307. https://doi.org/10.1016/j.scitotenv.2019.02.245

829   Jiao, J. J., Zhang, X., Liu, Y., & Kuang, X. (2015). Increased Water Storage in the Qaidam Basin,

830   the North Tibet Plateau from GRACE Gravity Data. PLoS One, 10(10), e0141442. https://doi.org/

831   10.1371.

832   Krishnaswami, S., Graustein, W. C., Turekian, K. K., & Dowd, J. F. (1982). Radium, thorium and

833   radioactive lead isotopes in groundwaters: application to the in situ determination of adsorption-

834   desorption rate constants and retardation factors. Water Resources Research, 6, 1663-1675.

835   Kuang, X., & Jiao, J. J. (2016). Review on climate change on the Tibetan Plateau during the last

836   half century. Journal of Geophysical Research Atmospheres, 121(8), 3979-4007. https://doi.org/

837   10.1029/WR018i006p01663

838   Kennedy, B. M., Lynch, M. A., & Smith, S. P. (1985). Intensive sampling of noble gases in fluids at

839   Yellowstone. I. Early overview of the data; regional patterns. Geochimica et Cosmochimica Acta,

840   49, 1251–1261. https://doi.org/10.1016/0016-7037(85)90014-6

841   Kennedy, B. M., & Matthijs, C.S. (2006). A helium isotope perspective on the Dixie Valley, Nevada,

842   hydrothermal system. Geothermics, 35(1), 26-43. https://doi.org/10.1016/j.geothermics.2005.09.

843   004

844   Kreutz, K. J., Wake, C. P., Aizen, V. B., Cecil, L. D., & Synal, H. A. (2003). Seasonal deuterium

845   excess in a TienShan icecore: influence of moisture transport and recycling in Central Asia.

846   Geophysical Research Letters, 30 (8). https://doi.org/10.1029/2003GL017896

847   Kong, Y. L., Wang, K., Pu, T., & Shi, X. (2019). Non-monsoon precipitation dominates groundwater

848   recharge beneath a monsoon affected glcacier in Tibetan Plateau. Jounral of Geophisical Research:

849   Atmospheres, 124(10), 10913-10930. https://doi.org/10.3390/w11061239

850   Klinger, Y., Xu, X. W., Tapponnier, P., Van, W. J., Lasserre, C., & King, G. (2005). High resolution

851   satellite imagery mapping of the surface rupture and slip distribution of the Mw 7.8, 14 November

852   2001 Kokoxili Earthquake, Kunlun Fault, Northern Tibet. Bulletin of the Seismological Society of

America, 95(5), 1970–1987. https://doi.org/10.1785 / 0120040233

Li, Z. X., Li Z. J., Feng, Qi., Zhang, B. J., Gui, J., Xue, J., & Gao, W. D. (2020). Runoff dominated by supra-permafrost water in the source region of the Yangtze river using environmental isotopes. Journal of Hydrology, 582. 125-140. https://doi.org/10.1016/j.jhydrol.2019.124506

Ma, J. Z., Ding, Z. Y., Edmunds, W. M., Gates J. B., & Huang, T. M. (2009). Limits to recharge of groundwater from Tibetan plateau to the Gobi desert, implications for water management in the mountain front. Journal of Hydrology, 364, 128–141. https://doi.org/10.1016/j.jhydrol.2008.10.010

Malard, A., Sinreich, M., & Jeannin, P. Y. (2016). Anovel approach for estimating karst groundwater recharge in mountainous regions and its application in Switzerland. Hydrological Processes, 30(13), 2153–2166. https://doi.org/10.1002/hyp.10765

Mark, D. (2003). Mountain and subpolar glaciers show an increase in sensitivity to climate warming and intensification of the water cycle. Journal of Hydrology, 282(1–4), 164-176. https://doi.org/10.1016/S0022-1694(03)00254-3

Morgenstern, U., Stewart, M.K., & Stenger, R. (2010). Dating of stream water using tritium in a post nuclear bomb pulse world: continuous variation of mean transit time with streamflow. Hydrology and Earth System Sciences, 14, 2289–2301. https://doi.org/10.5194/hessd-7-4731-2010

Pradeep, K. A., Joel, R. G., & Klaus, F. F. (2005). Isotopes in the water cycle: past, present and future of a developing science. Springer Netherlands. https://doi.org/10.1007/1-4020-3023-1

Post, V.E.A., Groen, J., Kooi, H., Person, M., Ge, S., & Edmunds, W. M. (2013). Offshore fresh groundwater reserves as a global phenomenon. Nature, 504, 71–78. https://doi.org/10.1002/hyp.10765

Phillips, F.M., Mills, S., Hendrickx, M.H., & Hogan, J. (2003). Environmental tracers applied to quantifying causes of salinity in arid-region rivers: results from the Rio Grande Basin, Southwestern USA. Elsevier, Developments in water science, 50, 327-334. https://doi.org/10.1016/S0167-5648(03)80029-1

Rangwala, I., Miller, J. R., Russell, G. L., & Xu, M. (2010). Using a global climate model to evaluate the influences of water vapor, snow cover and atmospheric aerosol on warming in the Tibetan Plateau during the twenty-first century. Climate Dynamics, 34(6), 859–872, https://doi.org/10.1007/s00382-009-0564-1

Sun, C. Y. (1991). Isotope hydrogeology in Golmud area. Qinghai Geology, 1, 26-31. https://doi.org/CNKI:SUN:GTJL.0.1991-01-003

884 Salamon, T. (2016). Subglacial conditions and Scandinavian Ice Sheet dynamics at the coarse-

885 grained substratum of the fore-mountain area of southern Poland. Quaternary Science Reviews, 151,

886 72–87. https://doi.org/10.1016/j.quascirev.2016.09.002

887 Sergey, A. S., & Vladimir, N. G. (2009). Snow isotopic content change by sublimation. Journal of

888 Glaciology, 55(193), 823-829. https://doi.org/10.3189/002214309790152456

889 Smerdon, B.D. (2017). Groundwater recharge: The intersection between humanity and

890 Hydrogeology. Journal of Hydrology, 555, 909–911. https://doi.org/10.1016/j.jhydrol.2017.10.075

891 Smerdon, B.D., Gardner, W. P., Harrington, G. A., & Tickell, S. J. (2012). Identifying the

892 contribution of regional groundwater to the baseflow of a tropical river (Daly River, Australia).

893 Journal of Hydrology, 464, 107–115. https://doi.org/10.1016/j.jhydrol.2012.06.058

894 Sun, Q. H., Miao, C. Y., & Duan Q.Y. (2015). Projected changes in temperature and precipitation in

895 ten river basins over China in 21st century. International journal of climatology, 35(6), 1125–1141.

896 https://doi.org/10.1002/joc.4043

897 Su, X., Xu, W., Yang, F., & Zhu, P. (2015). Using new mass balance methods to estimate gross

898 surface water and groundwater exchange with naturally occurring tracer 222Rn in data poor regions:

899 a case study in northwest China. Hydrological Processes, 29(6), 979–990. https://doi.org/10.1002/

900 hyp.10208

901 Tan, H. B., Chen, J., Rao, W. B., Zhang, W. J., & Zhou, H. F. (2012). Geothermal constraints on

902 enrichment of boron and lithium in salt lakes: an example from a river-salt lake system on the

903 northern slope of the eastern Kunlun mountains, China. Journal of Asian Earth Sciences, 51, 21-29.

904 https://doi.org/10.1016/j.jseaes.2012.03.002

905 Tolstinkhin, I., Lehmann, B. E., & Loosli, H. H. (1996). Helium and argon isotopes in rocks,

906 minerals, and related groundwaters: A case study in northern Switzerland. Geochimica et

907 Cosmochimica Acta, 60, 1497–1514. https://doi.org/10.1016/0016-7037(96)00036-1

908 Tan, H. B., Rao, W. B., Chen, J. S., Su, Z. G., Sun, X. X., & Liu, X. Y. (2009). Chemical and isotopic

909 approach to groundwater cycle in western Qaidam Basin, China. Chinese Geographical Science,

910 19(4), 357-364. https://doi.org/CNKI:SUN:ZDKX.0.2009-04-010

911 Tian, L. D., Yao, T.D., MacClune, K., White, J. W. C., Schilla, A., Vaughn, B., et al. (2007). Stable

912 isotopic variations in west China: a consideration of moisture sources. Journal of Geophysical

913 Research, 112 (D10). https://doi.org/10.1029/2006JD007718

914 Weiss, R. F. (1971). Solubility of Helium and neon in water and sea water. Jour. Chem. Eng. Data,

16, 235–241. https://doi.org/10.1021/je60049a019

Wang, Y.G., Guo, H.Y., Li, J., Huang, Y., Liu, Z.Y., Liu, C.E., et al. (2008). Investigation and Assessment of Grounderwater Resources and Their Environmental Issues in the Qaidam Basin. Geological Publishing House, 23-28.

Wang, Y., Wei, J. H., & Xie, H. W. (2018). The variation of terrestrial water storage in the Qaidam Basin based on GRACE data. South-to-North Water Transfers and Water Science & Technology, 01. https://doi.org/10.13476/j.cnki.nsbdqk.20180012

Wang, X., Yang, M., Liang, X., Pang, G., Wan, G., Chen, X., & Luo, X. (2014). The dramatic climate warming in the Qaidam Basin, northeastern Tibetan Plateau, during 1961–2010. International journal of climatology, 34(5), 1524–1537. https://doi.org/10.1002/joc.3781

Wang, Y. D., Zheng, J. J., Zhang, W. L., Li S.Y., Liu, X.W., Yang, X., & Liu, Y. H. (2012). Cenozoic uplift of the Tibetan Plateau: Evidence from the tectonice-sedimentary evolution of the western Qaidam Basin. Geoscience Frontiers, 3(2), 175-187. https://doi.org/10.1016/j.gsf.2011.11.005

Xiao, Y., Shao, J.L., Cui, Y.L., Zhang, G., & Zhang, Q.L. (2017). Groundwater circulation and hydrogeochemical evolution in Nomhon of Qaidam Basin, northwest China. Journal of Earth System Science, 126 (2), UNSP 26. https://doi.org/10.1007/s12040-017-0800-8

Xu, W., Su, X.S., Dai, Z.X., Yang, F.T., Zhu, P.C., Huang, Y. (2017). Multi-tracer investigation of river and groundwater interactions: a case study in Nalenggele River basin, northwest China. Hydrogeology Journal 25(7), 2015-2029. https://doi.org/ 10.1007/s10040-017-1606-0

Xiao, Y., Shao, J.L., Frape, S.K., Cui, Y.L., Dang, X.Y., Wang, S.B., & Ji, Y.H. (2017). Groundwater origin, flow regime and geochemical evolution in arid endorheic watersheds: a case study from the Qaidam Basin, northwest China. Hydrology and Earth System Sciences, 4381-4400. https://doi. org/ 10.5194/hess-2017-647.

Xiang, L., Wang, H., Steffen, H., Wu, P., Jia, L., Jiang, L., & Shen, Q. (2016). Groundwater storage changes in the Tibetan Plateau and adjacent areas revealed from GRACE satellite gravity data. Earth and Planetary Science Letters, 449, 228–239. https://doi.org/10.1016/j.epsl.2016.06.002

Yang, J.P., Ding, Y.J., & Chen, R.S. (2007). Climatic causes of ecological and environmental variations in the source regions of the Yangtze and Yellow rivers of China. Environ. Geol, 53, 113–121. https://doi.org/ 10.1007/s00254-006-0623-4

You, Q.L., Min, J.Z., & Kang, S.C. (2015). Rapid warming in the Tibetan Plateau from observations and CMIP5 models in recent decades. Int. J. Climatol., https://doi.org/10.1002/joc.4520

946 Yin, G.H., Shen, J., & Jiang, J.X. (2002). Tectonic background of the Ms 8.1 earthquake on 14 Nov,

947 2001 at east Kunlun fault. Arid Land Geography, 25(1), 24-29. https://doi.org/10.3969/j.issn.1001-

948 8956.2002.01.001

949 Ye, X.R., Tao, M.X., Yu, C.A., & Zhang, M.J. (2007). Helium and neon isotopic compositions in

950 the ophiolites from the Yarlung Zangbo River, Southwestern China: The information from deep

951 mantle. Science in China (Ser. D), 50 (6): 801–812. https://doi.org/10.1-007/s11430-007-0017-9

952 Yael, K., Yishai, W., Abraham, S., & Yoseph, Y. (2015). Application of radon and radium isotopes

953 to groundwater flow dynamics: An example from the Dead Sea. Chemical Geology, 411, 155–171.

954 https://doi.org/ 10.1016/j.chemgeo.2015.06.014

955 Zhou, H., Chen, L., Diwu, C.R., & Lei, C. (2018). Cenozoic uplift of the Qimantage Mountains,

956 northeastern Tibet: Contraints from provenance analysis of Cenozoic sediments in Qaidam Basin.

957 Geological Journal, 53, 2613–2632. https://doi.org/10.1002/gj.3.095

958 Zhang, G.L., Dong, J.W., Zhou, C.P., Xu, X.L., Wang, M., Ouyang, H., & Xiao, X.M. (2013).

959 Increasing cropping intensity in response to climate warming in Tibetan Plateau, China. Field Crops

960 Research, 142 , 36–46. https://doi.org/10.1016/j.fcr.2012.11.021

961 Zhao, L.J., Eastoe C.J., Liu, X.H., Wang, L.X., Wang, N.L., Xie, C., & Song, Y.X. (2018). Origin

962 and residence time of groundwater based on stable and radioactive isotopes in the Heihe River Basin,

963 northwestern   China.   Journal   of   Hydrology: Regional   Studies,   18,   31–49.

964 https://doi.org/10.1016/j.ejrh.2018.05.002

965 Zhu, Y.Z., Li, W.S., Wu, B.H., & Liu, C.L. (1989). New recognition on the geology of the Yiliping

966 Lake and the east and west Taijnar Lakes in the Qaidam Basin, Qinghai Province. Geological

967 Review ,35 (6), 558–565. https://doi.org/10.16509/j.georeview.1989.06.009

968 Zhao, Z.H., Wang, D.Q., Bai, Y.L., Yan, & C.H., Xu, X.F. (2019). Research on Establishing Tritium

969 Concentration Model of Precipitation in Northeast of Tarim Basin Based on Factor Analysis. Earth

970 and Environmental Science, 237(2), 022014 . https://doi.org/ 10.1088/1755-1315/237/2/022014

971 Zhu, X.H., Wang, W.Q., & Klaus., F. (2013). Future climate in the Tibetan Plateau from a statistical

972 regional climate model. J. Clim., 26(24), 10,125–10,138, https://doi.org/10.1175/JCLI-D-13-

973 00187.1